

# Research Progress in the Field of Tumor Model Construction Using Bioprinting: A Review

Jiachen Yu<sup>1,\*</sup>, Yingchun Zhang<sup>1,\*</sup>, Rong Ran<sup>2,\*</sup>, Zixiao Kong<sup>3</sup>, Duoyi Zhao<sup>1</sup>, Wei Zhao<sup>1</sup>, Yingxin Yang<sup>4</sup>, Lianbo Gao<sup>5</sup>, Zhiyu Zhang<sup>1</sup>

<sup>1</sup>Department of Orthopedics, the Fourth Affiliated Hospital of China Medical University, China Medical University, Shen Yang, 110032, People's Republic of China; <sup>2</sup>Department of Anesthesia, the Fourth Affiliated Hospital of China Medical University, China Medical University, Shen Yang, 110032, People's Republic of China; <sup>3</sup>China Medical University, Shen Yang, 110032, People's Republic of China; <sup>4</sup>General Hospital of Northern Theater Command, China Medical University, Shen Yang, 110032, People's Republic of China; <sup>5</sup>Department of Neurology, the Fourth Affiliated Hospital of China Medical University, China Medical University, Shen Yang, 110032, People's Republic of China

\*These authors contributed equally to this work

Correspondence: Zhiyu Zhang; Lianbo Gao, The Fourth Affiliated Hospital of China Medical University, No. 4 Chongshan Road, Huanggu District, Shenyang, Liaoning, People's Republic of China, Email [zyzhang@cmu.edu.cn](mailto:zyzhang@cmu.edu.cn); [lbhao@cmu.edu.cn](mailto:lbhao@cmu.edu.cn)

**Abstract:** The development of therapeutic drugs and methods has been greatly facilitated by the emergence of tumor models. However, due to their inherent complexity, establishing a model that can fully replicate the tumor tissue situation remains extremely challenging. With the development of tissue engineering, the advancement of bioprinting technology has facilitated the upgrading of tumor models. This article focuses on the latest advancements in bioprinting, specifically highlighting the construction of 3D tumor models, and underscores the integration of these two technologies. Furthermore, it discusses the challenges and future directions of related techniques, while also emphasizing the effective recreation of the tumor microenvironment through the emergence of 3D tumor models that resemble in vitro organs, thereby accelerating the development of new anticancer therapies.

**Keywords:** bioprinting, bioink, organoids, tumor spheroids, tumor chips

## Introduction

According to 2020 data, approximately 19.3 million new cancer cases were reported globally, resulting in around 10 million related deaths.<sup>1</sup> With the high incidence and mortality rates of cancer posing a serious threat to human health, there is an urgent demand for the development of more effective anticancer drugs. Nonetheless, the screening of such drugs remains a highly challenging and burdensome task due to these statistics.<sup>2</sup> Typically, tumor models are used to assess their anticancer effects, providing highly intuitive results.

The construction of tumor models has evolved from 2D to animal models and then to 3D models such as organoids, representing a gradual development. Although simple to use and economical, 2D cell culture models do not effectively replicate the in vivo environment. Animal models are widely used currently, offering a more complex biological environment. However, the major issue lies in the inevitable physiological differences between animals and humans, casting doubt on the reliability of the results.

Due to advancements in tissue engineering, bioprinting technology has emerged as a significant tool in the field of oncology. This technique involves the use of 3D printing to assemble cells, biomaterials, and growth factors in a precise and quantitative manner. The technology can create three-dimensional tumor tissue models that simulate the micro-environment of tumor occurrence and development. These models provide a more realistic representation of cell-cell and cell-matrix interactions, closely resembling the biological characteristics of in vivo tumors. This aids in the in-depth study of tumor growth, progression, metastasis, and other mechanisms, enabling rapid, high-throughput assessment of drug efficacy and toxicity, thereby facilitating personalized medicine. Today, 3D tumor spheroids, organoids, and tumor chips are successful products cultivated by the era. The combination of these tumor models with bioprinting technology

holds promise to provide faster and more accurate solutions for screening tumor treatment methods, ultimately benefiting millions of cancer patients. In simple terms, biological inks are synthesized from cells, bio-polymers, and other auxiliary components, followed by the use of appropriate bioprinting techniques to fabricate tumor models (Figure 1). This article provides an overview of the latest developments in bioprinting and 3D tumor models from a biomedical perspective, such as tumor spheroids, organoids, and tumor chips. We begin with a brief summary of the current state of size-based bioprinting technology, followed by a description of the latest advancements in closely related bioinks. Finally, we discuss tumor models in detail, outlining the challenges and prospects of bioprinting technology in the construction of tumor models.

## Overview of Bioprinting Technology

Bioprinting technology, as a crucial component of the two fundamental elements of bioprinting (bioprinting technology and bioinks), refers to the technique of creating three-dimensional objects by digitally controlled, continuous layer deposition of living cells and tissues as materials. From the earliest inkjet printing to the present, bioprinting technology has evolved into various forms and categories. The common ones we encounter include Inkjet bioprinting, Acoustic droplet ejection bioprinting, Laser-assisted bioprinting, Microfilament bioprinting, Stereolithography bioprinting, and Digital light processing (Figure 2). The classification can be based on the presence or absence of a nozzle, which includes nozzle-based jetting or extrusion printing, as well as nozzle-free, open-platform printing. To succinctly summarize these printing technologies, we have categorized existing techniques based on the additive manufacturing characteristics of

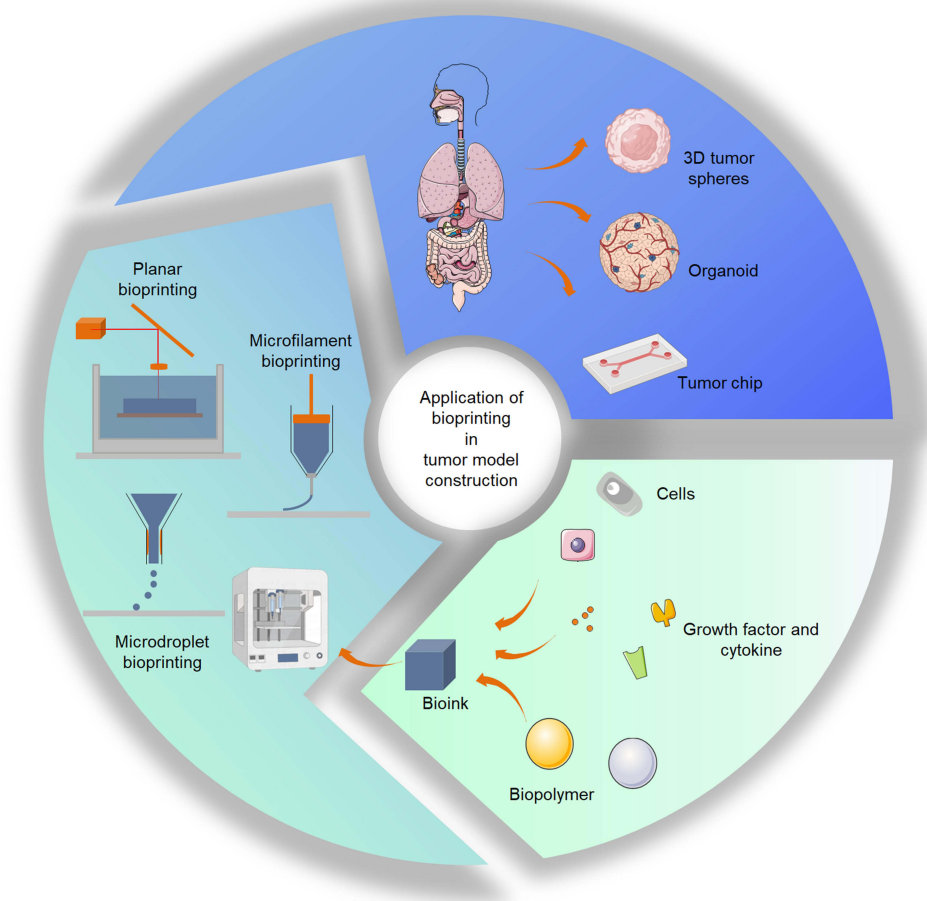


**Figure 1** Schematic diagram of bioprinting application in tumor model construction.

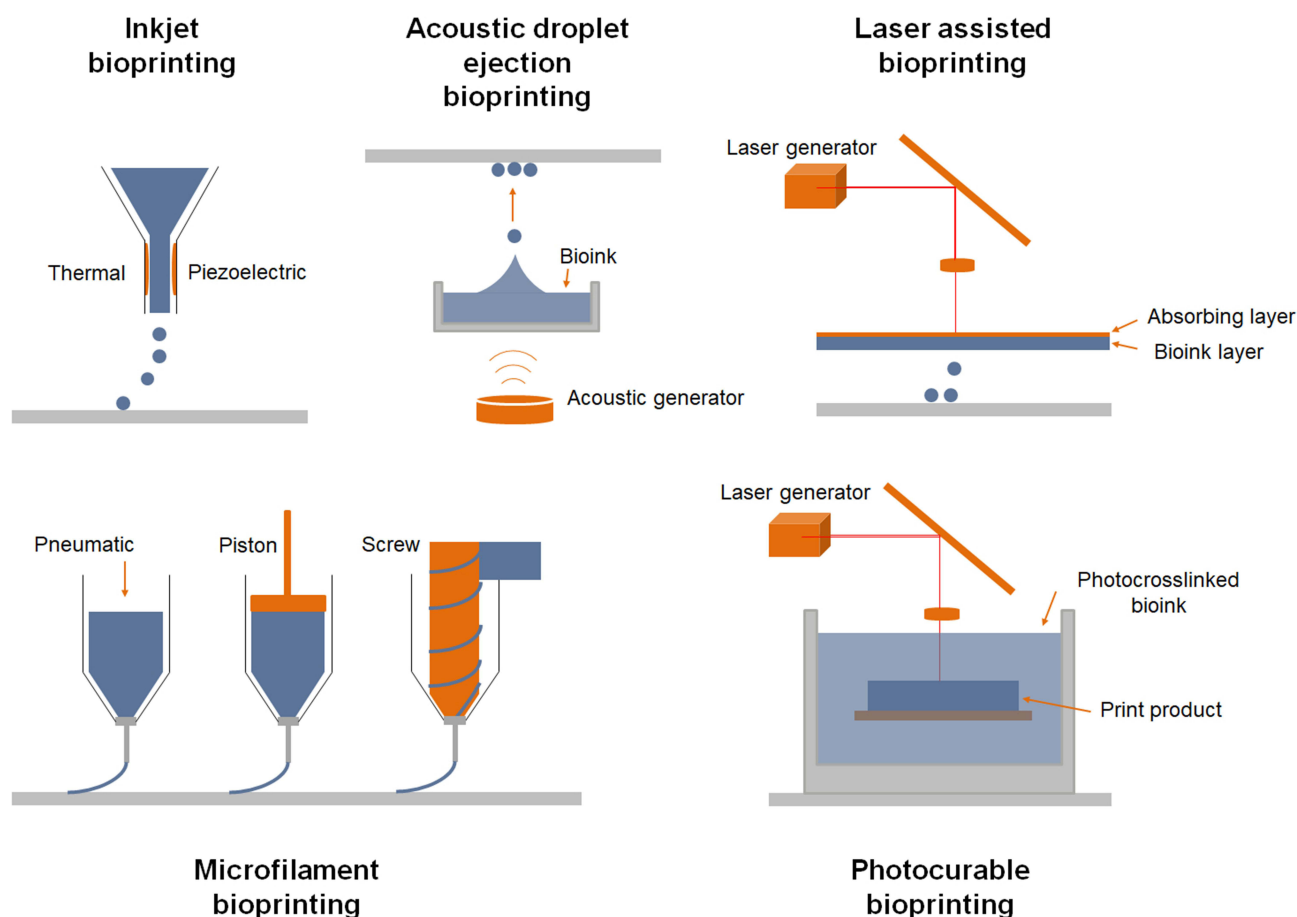


**Figure 2** Schematic diagram of bioprinting technology.

bioprinting, using the following classification: zero-dimensional droplet-based, one-dimensional filament-based, and two-dimensional plane-based (Table 1).<sup>3–5</sup>

## Zero-Dimensional Microdrop Bioprinting

This type of technology uses controllable cell-containing micro-drops as the structural forming unit, mainly including inkjet, acoustic, laser-assisted, and laser-induced transfer.<sup>6,15–17</sup> During the cell printing process, all four methods mentioned above have potential sources of cell damage, including thermal effects, tension from bubble rupture, instantaneous impact force during droplet ejection, and dehydration due to droplet evaporation. Overall, through effective process optimization, the micro-droplet-based printing process can achieve a cell survival rate of over 85%. In terms of shaping, the prominent advantages of these micro-droplet-based methods are high forming accuracy and fast printing speed, while the main drawback is the low ink viscosity, making droplet fixation difficult and thus challenging for forming larger complex three-dimensional structures.

Bioprinting using inkjet technology was first developed in 2003 and officially patented in 2006. This method is based on the traditional 2D inkjet printer, where the ink is replaced with bioink and the platform is switched to X-Y-Z control, enabling the 3D fabrication of biologically relevant objects. Bioink is deposited by controlled deformation of the nozzle's internal space as it flows through, driven by piezoelectric or digitally controlled thermal forces, causing the controlled volume to generate droplets through the nozzle. These droplets distribute the liquid onto a collection platform, forming layers in the z-direction to ultimately create a 3D object. Inkjet bioprinting has advantages such as a simple system and relatively low cost.<sup>18</sup> Multiple print heads can work in parallel, achieving high-resolution ( $\approx 30\ \mu\text{m}$ ) and fast manufacturing.<sup>19</sup> However, there are limitations to inkjet bioprinting, such as the

**Table 1** Advantages and Disadvantages of Bioprinting Technology

Dimensionality	Printing Technology	Advantage		Disadvantage		Cell Survival Rate	Reference
Zero- dimension	Inkjet printing	High molding accuracy and fast printing speed	The system is simple and the cost is relatively low	The viscosity of the ink is low, and it is difficult to shape the droplets, so it is difficult to form large complex three-dimensional structures		>85%	[6]
	Sonic printing		Simple structure, small manufacturing obstacles, compact size, non-contact operation, reduce the critical shear stress			>85%	[7]
	Laser-induced transfer printing		High cell viability		High cost	>95%	[8]
One-dimensional	Microfilament printing	Large scale complex structures can be formed, and natural or synthetic polymer materials with different crosslinking mechanisms and rheological properties can be formed. There is no cell damage caused by bubble rupture and instantaneous impact		The shearing effect of extrusion on cells is the main source of cell damage		40–80%	[9–11]
Two-dimensional	Stereolithography printing	Higher printing speed, high cell survival rate		Waste of ink, difficulty in structural detachment, oxygen inhibition, greater photostimulation and photoinitiator toxicity		>85%	[9,12]
	Digital light processing	Higher resolution, relatively faster printing speed, and flexibility in material selection.		Limited by the projection area of digital light projection, Digital light processing is typically used for printing smaller objects.		>95%	[13,14]

relatively low cell density ( $<10^6$  cells/mL) used for bioprinting and the ability to print only bioinks with viscosities in the range of 3.5–12 mPa s. Christensen et al successfully printed branched vascular structures using inkjet bioprinting by controlling and uniformizing the channel diameter.<sup>20</sup>

Bioprinters currently available with nozzles have limitations in printing resolution, as they are expected to cause clogging when the size is less than 100  $\mu\text{m}$ .<sup>21</sup> Additionally, decreasing the nozzle diameter increases shear stress during the printing process. When subjected to critical shear stress, mechanical damage to the printed cells may lead to cell death.<sup>22</sup> In order to address these drawbacks, Jentsch et al<sup>7</sup> introduced a novel 3D bioprinting technique based on the principle of acoustic droplet ejection (ADE). Ultrasonic signals emitted by transducers pass through a water tank, then through the bottom of a small coupling reservoir filled with a hydrogel suspension containing cells, ultimately producing ejected droplets containing cells. These droplets move upwards and adhere to a movable construction platform. This method eliminates the need for a nozzle, reducing critical shear stress. Numerical simulations indicate that the maximum shear stress in the ADE process is 2.7 times lower than that of a 150  $\mu\text{m}$  microvalve nozzle.

Laser-assisted bioprinting utilizes laser direct writing or laser induction forward transfer. The first application of laser-assisted printing to bioprinting was documented by Guillotin et al<sup>23</sup> in 2010, outlining bioprinting using micro-droplet arrays, setting the stage for its application in biomedicine. The system employing this technique typically comprises three layers from top to bottom: an energy absorption layer, a donor layer, and a bioink layer. The pivotal component in this system is the donor layer, which reacts to the applied laser beam. At the top of this donor layer is an energy absorption layer (such as titanium or gold), and at the bottom, a thin layer of bioink is suspended for bioprinting. When a selective laser beam is directed at the energy absorption layer, the corresponding area of the donor layer beneath it vaporizes, generating a high-pressure bubble at this interface. This pressure propels the bioink, leading to droplet deposition on the collection platform. By controlling the z-level of the collector, a 3D structure is eventually created. The advantage of laser-assisted bioprinting is that cells are not directly subjected to high shear stress. In fact, there is no contact between the dispenser and the bioink during the bioprinting process. Therefore, this bioprinting method can achieve a relatively high cell viability (>95%) and can deposit highly viscous substances (1–300 mPa.s). However, the main drawback of this



system is its high cost, primarily due to the necessity for a high-resolution and high-intensity laser diode. Additionally, concerns have been raised that using a laser beam to impact the basal layer may result in the release of metal particles, which could compromise the process's cell compatibility.<sup>8</sup>

## One-Dimensional Microfilament Bioprinting

This technology involves the utilization of one-dimensional gel microfilaments as the basic building block for bioprinting, specifically in reference to microextrusion-based 3D bioprinting. Microextrusion-based bioprinting stands as one of the earliest developed and most widely applied bioprinting techniques because of its capacity to construct intricate large-scale structures and to accommodate the creation of natural or synthetic high molecular weight polymer materials with varied crosslinking mechanisms and rheological properties.<sup>9</sup> Unlike droplet-based printing methods, microextrusion-based methods do not suffer from issues such as bubble bursting or instantaneous impact that can cause cell damage. The main source of cellular injury from this method is the shearing action on the cells during the extrusion process, especially when the ink material has a high viscosity,<sup>10,11</sup> as shown by data demonstrating a 13% decrease in cell viability after printing.<sup>24</sup>

The fundamental mechanism of using extrusion for 3D bioprinting in the field of biology was first described by Iwan et al in 2002.<sup>25</sup> Similar to the classic fused deposition modeling (FDM) process, this technique involves the extrusion of materials into filaments, which are then layered to construct a structure. Two main fluid distribution systems have shown high performance in bioprinting applications: pneumatic and mechanical drives.<sup>3</sup> Pneumatic systems can be valveless or valve-based, with valveless systems being more straightforward to fabricate and thus being the most commonly used in bioprinting.<sup>26</sup> Valve-based systems offer various advantages in terms of pressure and pulse frequency control, enabling precise material deposition and high-resolution bioprinting. Mechanical systems are primarily driven by pistons or screws. Piston-based systems enable direct control over the deposition of bioink onto the platform. Screw-driven systems are better suited for high-viscosity bioink due to their improved spatial control, but they may pose a risk to cells due to the increased pressure drop at the nozzle outlet.<sup>26</sup>

In comparison to previously mentioned platforms, extrusion-based bioprinting offers several benefits, such as the capability to deposit high-viscosity bioink (30 mPa s to  $> 6 \times 10^7$  mPa.s) and higher cell density ( $> 10^8$  cells/mL to cell spheroids).<sup>9,27</sup> Extrusion-based bioprinting systems have the capacity to continuously and consistently extrude bioink, making them more suitable for most applications due to the preservation of the printed tissue structure. As cells undergo significant shear stress during the extrusion process, the typical cell viability after extrusion-based bioprinting ranges around 40–80%.<sup>9</sup>

The driving force solves the problem of the dynamic source of microfilament extrusion, while the formation of microfilaments and other process treatments directly affect the quality of the final printed product. In the formation of microfilaments and forming structures, the ink materials generally undergo gelation or crosslinking. Pre-crosslinking treatment is used to partially crosslink the ink before printing to facilitate direct extrusion into filaments. Temperature control treatment is used for various thermosensitive ink materials and adopts targeted heating or cooling treatments to achieve the desired filament formation effect.<sup>28,29</sup> Post-crosslinking treatment takes on various forms, with the general principle that the extruded ink is crosslinked into filaments at the nozzle tail end, such as the simultaneous injection of ink and crosslinking agents, coaxial injection, atomization treatment, and direct printing in a crosslinking agent solution, etc., with these different forms of treatment widely used in sodium alginate hydrogel printing.<sup>30–32</sup> As a new approach to enhance the resolution of current bioprinting platforms, electrospinning technology makes use of the electrostatic properties of microfilaments. This method employs rapid stretching of charged polymer solutions or melt jetting, together with solvent evaporation and solidification, and then collects the filaments as fiber mats.<sup>33</sup> Following the application of voltage between the syringe and collector, the solution ejected from the metal needle transforms into a charged jet, which is then drawn towards the collector. As the solvent evaporates during the journey from the syringe to the collector, the diameter of the jet reduces significantly, leading to the production of numerous fibers deposited on the metal collector. Recent advancements in electrospinning technology have enabled the production of finer-diameter fibers, making it a promising method for enhancing the resolution of existing bioprinting platforms. Typically, the equipment comprises an X-Y-Z robot workbench and a standard electrospinning device, incorporating a solution or molten polymer extrusion

system equipped with an injection pump or pneumatic regulator, as well as a high-voltage power supply.<sup>34–36</sup> Electrospinning allows for the control of bioprinting in a continuous or intermittent manner. One of the primary challenges in printing electrospun fibers is addressing the erratic oscillations of charged jets, which can lead to unstable fiber and structure formation.<sup>37</sup>

## Two-Dimensional Planar Bioprinting

Stereolithography (SLA) and Digital Light Processing (DLP) are two commonly used photopolymerization techniques in the field of bioprinting. Both utilize a light source to cure liquid photosensitive resins and can complete the bioprinting process on a two-dimensional plane. However, there are some differences in their technical implementation and application characteristics. Each technology has its own advantages, and the choice between SLA and DLP depends on the specific application requirements. SLA is more suitable for manufacturing parts that require extremely high precision, while DLP is ideal for the rapid printing of small, delicate structures. In the field of bioprinting, both of these technologies are employed in the fabrication of biocompatible scaffolds and tissue models.

The origins of stereolithography for additive manufacturing can be dated to 1984, when Charles W. Hull outlined the process of creating 3D objects by selectively converting the physical state of fluid in a resin layer into a solid through layer-by-layer photopolymerization.<sup>38</sup> Stereolithography technology utilizes a laser beam to scan liquid photosensitive resin point by point, constructing each layer one point at a time. This method allows for very precise control over the curing process and is suitable for the fabrication of high-precision components. However, due to the point-by-point curing nature, the printing speed of SLA is generally slower and it is not ideal for mass production. In the medical field, the earliest use of stereolithography involved the production of models for cranial surgery, enabling researchers to generate highly precise and detailed skull models.<sup>39</sup> This technology refers to stereolithography for cell printing, which is suitable for photocrosslinking bioinks. During printing, a photocrosslinking light source is projected onto the bioinks through a digital projector, selectively solidifying the bioinks layer by layer through photopolymerization, with the process controlled by a movable workstation along the Z-axis. By projecting 2D images onto the bioink reservoir, stereolithography allows for the creation of intricate 3D structures without the need for the printing head to move along the x-y direction. This characteristic leads to a faster bioprinting speed, potentially surpassing that of droplet and filament-based methods.<sup>12</sup> Within the area exposed to light, the ink selectively gels based on the digital model, leading to the layered stacking necessary for creating a three-dimensional structure.<sup>40,41</sup> As one of the earliest invented 3D printing technologies, it is widely applied in the field of rapid prototyping. High cell viability (>85%) is achieved by bioprinters through the selective photocrosslinking of bioinks, which avoids subjecting the cells to shear stress.<sup>9</sup> For direct cell printing, apart from ink wastage, difficulty in structural detachment, and oxygen inhibition, it may also cause significant light stimulation and photoinitiator toxicity to the cells. Additionally, the limitation of ink material types is a drawback of this technology. One drawback of this system is the requirement for the liquid to be transparent and for limited scattering; otherwise, the material will not be uniformly penetrated by the light, resulting in uneven crosslinking.

Stereolithography technology has been improved by integrating a digital micromirror device (DMD) into the laser optical path, enabling the entire layer to be cured at once without the need for point-by-point scanning. The DMD, composed of many micro-mirrors, can rapidly switch between on and off states. Based on the loaded image information, the DMD precisely controls the reflection of light through the optical system and irradiates the photosensitive resin surface in a specific pattern, achieving rapid curing of the target area. DLP technology uses a digital micromirror array (DMD) to project light patterns, thereby curing photosensitive resins. This method allows for precise control of the curing area by changing the projected light patterns, enabling the printing of complex structures. With a high resolution and faster printing speed due to the simultaneous curing of the entire layer, DLP is suitable for batch production. Moreover, DLP technology can operate over a broader range of light wavelengths, increasing the flexibility of material selection and the diversity of applications.<sup>13</sup> These advantages make DLP technology widely applicable in bioprinting and other high-precision 3D printing fields.

Tang et al<sup>42</sup> used digital light processing (DLP) technology for rapid bioprinting, constructing a mixed cell model containing patient-derived glioblastoma stem cells (GSCs), macrophages, astrocytes, and neural stem cells (NSCs). For the first time, they simulated the complex microenvironment of glioblastoma in vitro, including the infiltration of immune

cells and the interaction between tumor cells and normal brain tissue. This demonstrated the versatility of the bioprinted model in simulating the tumor microenvironment, including the invasiveness of tumor cells, drug resistance, and immune interactions. Mei et al<sup>43</sup> bioprinted a non-small cell lung cancer (NSCLC) model using DLP technology and simulated the human vascular system within the model. They precisely constructed a three-dimensional lung cancer model with central blood vessel channels using a bioink composed of methacrylated gelatin (GelMA). This model not only included simulated blood vessel structures but also featured an inlet and outlet to connect to a perfusion system that could supply nutrients and oxygen through a peristaltic pump, simulating the flow of blood in the human body. In the study by Ma et al,<sup>14</sup> live/dead cell staining tests conducted 1 and 7 days after printing with DLP technology showed that the cell viability was greater than 95%, indicating that the DLP printing process did not harm the cell survival rate.

## Bioink Design

Bioinks are a special type of ink used in the field of bioprinting, composed of multiple components including cells, cell scaffolds, and other auxiliary ingredients<sup>44,45</sup> (Table 2). The following are common components found in bioinks: Cells: Bioinks typically contain a variety of cells, such as stem cells, fibroblasts, chondrocytes, etc. The selection of cells depends on the specific application purpose and the type of tissue to be constructed. Cell scaffolds: These are usually biodegradable bio-polymers, such as gelatin, alginate, etc., which are often present in bioinks. These bio-polymers provide structural support for cell adhesion and assist in forming the desired three-dimensional structures during the bioprinting process. Additionally, to promote cell growth and differentiation, other components such as growth factors and cytokines, including fibroblast growth factor (FGF) and vascular endothelial growth factor (VEGF), may be incorporated into the bioink. These elements mimic natural biological signals, enhancing cell viability and tissue regeneration. It is worth noting that the specific composition of bioinks can be customized and improved according to different research and application needs. Researchers can choose the appropriate combination of ingredients to prepare bioinks based on the target tissue structure, cell characteristics, and requirements of the printing equipment. Moreover, the formulations and preparation methods of bioinks are continuously evolving and improving to enhance printing performance and cell viability.

**Table 2** The Composition of Bioink

The composition of Bioink	Classification	Example	Characteristic	Reference
Cells	Existing cell line	HeLa cells, K7M2 cells	It can be cultured in vitro for a long time and is easily obtained	
	Patient primary cells	It is isolated after tumor resection and subjected to limited in vitro expansion before being used to build tumor models	Personalized tumor models can be made	
	Stem cell	Bone marrow mesenchymal stem cells	Simulation of tumor initiation and progression, simulation of tumor heterogeneity, suitable for long-term culture and expansion	[46]
Cell scaffolds	Natural and synthetic hydrogels	Alginate, silk protein, gelatin, collagen, chitosan, agarose, hyaluronic acid	Easy to obtain and prepare, with good biocompatibility	[47–52]
	dECM Bioink	Formulated using fat, cartilage and heart tissue	Contains important non-cellular components such as growth factors, providing a superior microenvironment for the growth of specific tissues	[53]
Other auxiliary components	Growth factor	Fibroblast growth factor (FGF) Transforming Growth factor- $\beta$ (TGF- $\beta$ ) Vascular endothelial growth factor (VEGF)	Can directly or indirectly affect cell behavior and tissue development	[54–56]

## Cells in Bioink

In the construction of tumor models using bioinks, there are various options for cell sources based on the research or experimental objectives. Established cell lines, commonly referred to as cell lines, are a popular choice for cell sources because they can be cultured *in vitro* for extended periods and are readily available. Examples of commonly used tumor cell lines include HeLa cells and K7M2 cells, which originate from different types of tumors and can be selected for cultivation and use according to specific needs. Patient-derived primary cells: To more closely simulate the actual tumor environment, researchers may choose to use primary cells obtained from tumor patients (typically mature, terminally differentiated cell types). These cells can be isolated after resection and undergo limited *in vitro* expansion before being utilized to construct tumor models. This cell source retains the biological characteristics of the original tumor, enabling the creation of personalized tumor models. However, due to the complexity of their tissue origin, there may be variations in cell types and biological properties. Stem cells, with their potential for self-renewal and multilineage differentiation, can also serve as a cell source for constructing tumor models. Stem cells, with their capacity for self-renewal and differentiation, can mimic the behavior of tumor-initiating cells, which are often responsible for tumor initiation, progression, and recurrence. They can also generate cell populations containing various stages of differentiation, thereby better simulating the heterogeneity within tumors.<sup>57</sup> As an alternative solution to address the limited availability of cells, mesenchymal stem cells from adult bone marrow are among the most commonly used stem cells.<sup>46</sup> They have the ability to differentiate into various tissue types and can be expanded and differentiated into mesenchymal tissues such as bone, cartilage, tendon, fat, and bone marrow stroma both *in vitro* and *in vivo*.<sup>58</sup> Furthermore, stem cells derived from perinatal or amniotic sources can also be expanded and differentiated into multiple cell lineages, including adipocytes, osteoblasts, myogenic cells, endothelial cells, neuronal cells, and hepatocytes, thus serving as an alternative source of multipotent cells.<sup>59</sup>

For constructing tumor models using bioinks, there are several options for cell sources depending on the research or experimental objectives. Established cell lines, known as cell lines, are a common choice for cell sources because they can be cultured *in vitro* for extended periods and are easily accessible. Commonly used tumor cell lines include HeLa cells, K7M2 cells, etc., derived from different types of tumors, and can be selected for cultivation and use based on specific needs. Patient-derived primary cells: To closely simulate the real tumor environment, researchers may opt to use primary cells obtained from tumor patients (usually mature, terminally differentiated cell types). These cells can be isolated after resection and undergo limited *in vitro* expansion before being used to construct tumor models. This cell source retains the biological characteristics of the original tumor, achieving personalized tumor models; however, due to the complexity of tissue origin, there may be variations in cell types and biological properties. Stem cells, which have the potential for self-renewal and multipotent differentiation, can also serve as a cell source for constructing tumor models. Stem cells, with their ability to self-renew and differentiate, can be used to simulate the behavior of tumor-initiating cells, which are typically responsible for the initiation, progression, and recurrence of tumors. They can also generate cell populations containing different stages of differentiation, thereby better simulating the heterogeneity within tumors.<sup>57</sup> As an alternative solution to the limited availability of cells, mesenchymal stem cells from adult bone marrow are the most commonly used stem cells.<sup>46</sup> They can differentiate into various tissue types and can be expanded and differentiated into mesenchymal tissues such as bone, cartilage, tendon, fat, and bone marrow stroma *in vitro* or *in vivo*.<sup>58</sup> Additionally, stem cells derived from perinatal or amniotic sources can also be expanded and differentiated into multiple cell lines, including adipocytes, osteoblasts, myogenic cells, endothelial cells, neuronal cells, and hepatocytes, thus serving as an alternative source of multipotent cells.<sup>59</sup>

## Cell Scaffolds in Bioink

Tissues are not composed of a single type of cell. The function of the liver primarily relies on hepatocytes, but other essential cells such as cholangiocytes, hepatic stellate cells, and Kupffer cells are also crucial. In the brain, billions of neurons are surrounded by astrocytes, which provide necessary nutrients to neurons and contribute to immune modulation.<sup>60,61</sup> Human tissues are typically composed of cells, extracellular matrix (ECM), various growth factors and bioactive molecules, all existing in a complex and coordinated manner.<sup>60,62,63</sup> The extracellular matrix (ECM) is a complex network of macromolecules synthesized and secreted by various tissues and cells in the body, including

fibroblasts, mesenchymal cells, and epithelial cells. These molecules are distributed and accumulate in the cell surface and interstitial substances. The ECM forms the cellular scaffold of tissues and organs, providing a microenvironment for cell survival and growth. It significantly influences cell adhesion, differentiation, proliferation, migration, and functional expression. Natural and synthetic hydrogels have the capacity to mimic the microenvironment of human tissues, with good biocompatibility that promotes the exchange of nutrients and waste with cells and can partially restore ECM functions, making them ideal materials for cell scaffolds.<sup>64</sup>

Over the past few decades, several natural and synthetic hydrogels have shown great potential as cell scaffolds in bioprinting. Alginate, silk fibroin, gelatin, collagen, chitosan, agarose, and hyaluronic acid have all been extensively studied as bio-inks for cell scaffolds.<sup>47</sup> These cell scaffolds exhibit a range of sensitive properties, including ionic sensitivity, photopolymerization, thermosensitivity, enzymatic sensitivity, and pH sensitivity, allowing simple gels to form solid 3D structures before, during, or after the bioprinting process. Alginate is a commonly used bio-ink component in medical and bioprinting applications due to its adhesive properties and straightforward calcium chloride crosslinking mechanism, making it an attractive material for bioprinting.<sup>48,49</sup> However, its chemical structure often hinders cell adhesion, requiring the addition of other natural polymers, such as gelatin-based materials, collagen, or silk fibroin, to induce cell adhesion and bioactivity.<sup>51</sup> Gelatin and methacrylated gelatin (GelMA) are also widely used in bioprinting due to their excellent cell compatibility and mechanical properties.<sup>50</sup> However, the use of GelMA requires photoinitiators for crosslinking and solidification, which may be toxic to cells at high concentrations.<sup>51</sup> Similarly, hyaluronic acid and chitosan, due to their biodegradability and good biocompatibility, can be modified into printable cell scaffolds for the construction of cell-loaded structures, providing tunable performance and mechanical properties.<sup>52,65</sup>

At the macroscopic level, synthetic materials offer superior physical properties, enabling the manipulation of the mechanical, structural, and geometric characteristics of bioinks, including elastic modulus, tensile strength, porosity, and alignment. In contrast, natural materials provide an appropriate structural and biochemical environment for cell encapsulation and positioning. We need a material that can combine the advantages of both types of materials while closely replicating the structure and environment of human tissues. A successful bioprinting material should possess the following characteristics: printability, biocompatibility, mechanical properties, and shape and structure. (1) Printability: The material should be suitable for deposition during the printing process, with appropriate viscosity, shear properties, response transition times, and suitable sol-gel transition stimuli. Extrusion-based techniques typically require materials with higher viscosity and shear thinning properties, while inkjet-based techniques require low viscosity materials with very short sol-gel response and transition times. (2) Biocompatibility: In the field of bioprinting, bioinks must have appropriate degradability, support cell adhesion, and not cause severe immune reactions or toxicity.<sup>66</sup> (3) Mechanical properties: The mechanical properties of bioinks in terms of stiffness, elasticity, and strength should be consistent with the target tissue's mechanical properties. (4) Shape and structure: The printed structures should closely resemble the shape and structure of natural tissues.

Compared to hydrogels with more uniform compositions, the ECM in the body is secreted and composed of many cells. Specifically, cells release specific molecules and proteins in the appropriate environment, which aggregate to form the ECM. This includes collagen, fibronectin, proteoglycans, and bone matrix proteins, among others.<sup>67</sup> During the ECM secretion process, cells selectively release specific ECM molecules based on their environment and functional needs. These molecules form a three-dimensional structure on the cell surface, providing support and influencing the environment for cell morphology, differentiation, and function. The ECM also regulates biological processes such as cell signaling, cell-cell interactions, and cell migration. Notably, the composition of ECM components secreted by different types of cells may vary depending on the cell type and the tissue or organ in which they are located. For example, in bone tissue, osteocytes secrete an ECM rich in collagen and bone matrix proteins, while in connective tissue, fibroblasts secrete an ECM rich in collagen. Various sources, such as dermis, bladder, small intestine, mesothelium, pericardium, heart valves, and different species, can provide ECM.<sup>68</sup> Nagao et al<sup>69</sup> identified methods for extracting hydrogels from human renal cortex. Compared to normal renal tissue, this renal ECM (K-ECM) hydrogel contains a large amount of natural matrix proteins, providing niches that simulate the natural microenvironment of the respective bodies (Nagao et al, 2016). Bi et al recently discovered that liver-derived ECM (L-ECM) obtained from pigs can induce the differentiation of rat mesenchymal stem cells into hepatocytes.<sup>70</sup> In the construction of tumor models, it is crucial to



retain non-cellular components such as growth factors, which play an important role in cell growth, differentiation, migration, and tissue regeneration. For example, fibroblast growth factor (FGF) can promote cell proliferation and neovascularization, which is essential for tissue repair and regeneration, and the state of FGF can affect the rate of tumor progression.<sup>54</sup> Transforming growth factor- $\beta$  (TGF- $\beta$ ) is responsible for regulating cell proliferation, differentiation, and migration, and is also involved in tissue remodeling and fibrosis processes, which can slow down tumor progression under certain conditions.<sup>55</sup> Vascular endothelial growth factor (VEGF) specifically promotes the proliferation of vascular endothelial cells and the formation of new blood vessels, which is crucial for vascularization in tissue engineering. In the study by Jain et al,<sup>56</sup> inhibition of VEGF led to a reduction in vascular permeability, thereby increasing the delivery of oxygen and therapeutic drugs to tumors. These growth factors and cytokines are usually present in bioinks in an active form and can directly or indirectly influence cell behavior and tissue development. By precisely controlling the release and concentration of these factors, bioinks can provide an optimized growth environment for specific tissue engineering applications.

Decellularized extracellular matrix (dECM) is a natural scaffold produced by removing cellular components from tissues or organs while retaining their three-dimensional structure and some native fibrous components, such as collagen fibers. Due to its natural biocompatibility, tissue specificity, and ease of fabrication into usable bioinks, dECM is gaining increasing attention.<sup>71</sup> Simple hydrogel preparation does not possess these advantages. dECM derived from various tissues has been shown to serve as a bioink for 3D bioprinting. Jang and colleagues<sup>53</sup> created innovative tissue-specific dECM bioinks using adipose, cartilage, and cardiac tissues. Specific cells from each tissue type were able to proliferate for at least 14 days in these tissue-specific bioinks. These cell-laden dECM bioinks can be deposited through extrusion from a nozzle and then gelate at physiological temperatures to maintain the generated 3D structures. These bioinks immediately gelate at 15°C and form a stable crosslinked hydrogel within 30 minutes at 37°C, without the need for any stringent crosslinking conditions or gelation additives. Overall, dECM is a promising biomaterial that can serve as an essential component of bioinks, providing an optimized microenvironment for the growth of specific tissues, including but not limited to cartilage, cardiac, adipose, and liver tissues. Bioinks derived from ECM offer unparalleled biocompatibility, providing a favorable environment for tissue regeneration. The gel-like natural biomaterials are conducive to encapsulating cells and growth factors. In cell printing technology, various types of printers are typically used to directly print the corresponding structures with bioinks. However, their limited mechanical properties pose a challenge to their contribution to the physical properties of tissues, making the 3D shape of printed structures composed solely of hydrogels very challenging.<sup>72</sup> Nevertheless, bioinks can be crosslinked and modified chemically to alter their mechanical strength or degradation time.<sup>73</sup>

Bioinks generally need to meet various criteria. For instance, the viscosity must be low enough to be extruded through a printing head while preventing high shear rates within the loaded units, but it should also be high enough to maintain the 3D shape after extrusion. These requirements have led to a significant focus on shear-thinning hydrogels in many bioprinting applications. Shear-thinning hydrogels exhibit low viscosity under high shear stress and return to their original viscosity once the shear stress is removed.<sup>3,74</sup> The addition of supplements like graphene nanosheets can significantly enhance the tensile strength of soft hydrogels.<sup>75</sup> The incorporation of a small amount of graphene (0.1–0.3 wt%) into chitosan can increase the elastic modulus of chitosan by about 200%. In vitro colorimetric and cell adhesion test results indicate that chitosan with graphene still possesses good biocompatibility. Beyond the passive effects on loaded cells through mechanical forces, bioinks should also directly influence cell survival and behavior. The biological properties and biocompatibility of bioinks play a crucial role in ensuring the generation of the desired tissue. The performance of an ideal bioactive hydrogel scaffold should reflect the structural and biological characteristics of natural tissue ECM. Currently, hydrogels still face significant challenges in replicating the diverse biological functions and mechanical properties of ECM.

## Overview of Tumor Model Construction

From a temporal perspective, the development of tumor models can be broadly categorized into three types: two-dimensional cell culture models, animal models, and models that can replicate the tumor microenvironment.



(1) Two-dimensional cell culture models (Time span: early 20th century to present): The earliest tumor models involved the growth of cancer cells in two-dimensional cell culture dishes. These models were used to study the fundamental processes of cell growth, metabolism, and the effects of drugs on cells. However, 2D cell culture models have limited capabilities in simulating the complex tumor microenvironment within the human body, and struggle to replicate the diverse phenotypes,<sup>76</sup> gene and protein expressions,<sup>77</sup> and in vivo drug responses<sup>78</sup> of cancer cells under 2D conditions.

(2) Animal models (Time span: 1950s to present): To gain a comprehensive understanding of tumor development and assess the effectiveness of new therapeutic methods, scientists began using animal models, such as mice and rats. Even today, animal models remain the benchmark for drug screening and cancer research, providing a more complex and realistic physiological environment for studying tumor growth, metastasis, and treatment responses. Animal models offer insights into more complex biological environments, whole-system responses, and in vivo drug metabolism and side effects. However, these models still fail to faithfully replicate the essential elements of the human tumor microenvironment (TME). The extensive use of animals in laboratory research has also raised ethical concerns, emphasizing the need for alternative methods to more accurately and clinically relevantly recreate the in vivo TME. Specifically, they only provide the mouse physiological microenvironment for human tumor cells, lacking key features of natural human organ and biological system functions. Moreover, the compromised immune system in mice may affect cancer progression, reducing their reliability in drug testing.<sup>79</sup> To address these challenges, humanized mouse models have recently been developed, utilizing gene-editing technologies to study the interaction between cancer and the human immune system.<sup>80</sup>

(3) The tumor model replicates the tumor microenvironment (Time span: 1970s to present): The extracellular matrix (ECM) provides structural support for cells. In the context of the tumor microenvironment, the ECM plays a crucial role in controlling the behavior and interactions of tumor cells. As a component of the human tumor microenvironment (TME), the ECM interacts with tumor cells, immune cells, and other factors, influencing tumor formation and progression. The TME is a multifaceted environment, including tumor cells and surrounding non-cellular components, such as immune cells, blood vessels, fibroblasts, and matrix molecules. To accurately create corresponding tumor models in vitro, we must strive to replicate the tumor microenvironment as much as possible. To better simulate the real growth environment of tumors, scientists have begun to culture tumor cells in a way that captures their essence. Among these are the most representative 3D tumor spheroids, organoids, and tumor chips (Table 3), which are three different but interconnected technologies, each with unique applications yet overlapping and

**Table 3** The Tumor Model Replicates the Tumor Microenvironment

The Tumor Model Replicates the Tumor Microenvironment	Classification	Time Span	Characteristic	Specific Techniques and Methods	Reference
3D tumor spheroids	Scaffold-Free 3D tumor spheroids	Early 20th century to present	Simplified culture conditions; High cell density; Formation of hypoxia and metabolic gradient; High throughput screening	Specially designed culture plates (eg, low adhesion or non-adhesion surfaces) or specific culture techniques (eg, hanging drop method, rotary culture method) are often used to promote the formation of spheroids	[82,83]
	Scaffold-Based 3D tumor spheroids	Early 20th century to present	Good biocompatibility; Simulate the internal environment; Structural stability; It can simulate cellular interactions; Drug delivery studies may be conducted	Support cell growth and tissue formation by using natural or synthetic biological materials (such as extracellular matrix, hydrogels, etc.) as scaffolds	[84]
Organoid		1950s to present	Stable three-dimensional structure; It contains multiple cell types that can simulate the complexity of the tumor microenvironment	The shape, size, and composition of organoids can be precisely controlled using micropatterns, microfluidic chips, or bioprinting	[85–87]
Tumor chip		1970s to present	Microfluidic channels provide a dynamic culture environment for tumor cells. Can simulate the tumor microenvironment; Multi-parameter monitoring is possible	Microfluidic technology was used to simulate the tumor microenvironment. 3D tumor structures were formed using bioprinting techniques. Data can be monitored in real time by integrating micro-sensors on the chip	[88–90]

complementary relationships.<sup>81</sup> These tumor models allow for better simulation of the interactions between tumor cells within tissues and multicellular tissue structures, providing more physiologically relevant models that can offer a more realistic and accurate representation of the tumor microenvironment, aiding in the study of tumor formation, growth mechanisms, and drug responses. Three-dimensional tumor spheroids partially replicate the tumor microenvironment, allowing for better simulation of the interactions between tumor cells within tissues and multicellular tissue structures, providing more physiologically relevant models. Organoid models capture the essence of tumors at the organ level, offering a dynamic 3D model that can provide deeper insights into the mechanisms of tumor progression and has shown great potential in cancer drug screening. Tumor chips are a microfluidic technology that studies the physiological and pathological processes of organs by constructing microenvironments simulating human organs on microchips. Bioprinting technology allows for the precise 3D arrangement of cells and support structures, thereby simulating complex tumor tissues. There is a close connection between these three technologies. For example, 3D tumor spheroids can serve as the basic units for constructing tumor chips and organoids to simulate the tumor microenvironment and study tumor biological characteristics. At the same time, the development of organoid and tumor chip technologies also provides new tools and methods for the study of 3D tumor spheroids, such as precisely controlling culture conditions through microfluidic technology to enhance the physiological relevance and application range of 3D tumor spheroids.

In summary, driven by continuous advancements in science and technology and our understanding, the construction of tumor models has evolved from two-dimensional cell cultures to animal models, and now to organoids and other tumor models that can replicate the tumor microenvironment.

### 3D Tumor Spheroids

The 3D tumor spheroid is a model of three-dimensional cell culture utilized to mimic tumor tissues *in vitro*, created through the aggregation of cancer cells in a 3D cell culture environment. In contrast to conventional 2D cell culture models, this three-dimensional structure offers a more faithful representation of cell-cell interactions, cell-matrix interactions, and responses to external signals within tumor tissues. These spheroids can replicate cell-cell interactions,<sup>91</sup> growth kinetics, and the deposition of new ECM similar to human solid tumors.<sup>92</sup> Furthermore, accumulating evidence indicates that the dense ECM deposition and strong cell-cell contact within tumor spheroid aggregates can establish physical barriers resembling those present in the body, hindering the infiltration of drugs and immune cells, thus mirroring chemoresistance.<sup>93</sup> By virtue of their tumor-like characteristics, tumor spheroids have become established models for drug screening, with the goal of reducing drug development expenses and unnecessary animal experimentation.<sup>94,95</sup>

#### Scaffold-Free 3D Tumor Spheroids

Scaffold-Free 3D tumor spheroids do not rely on external scaffold materials but instead naturally form spheroid structures through the inherent adhesion and proliferation capabilities of cells. These models typically utilize specially designed culture plates (such as low-adhesion or non-adhesive surfaces) or specific culture techniques (such as the hanging drop method, rotating culture) to facilitate spheroid formation.<sup>82</sup> These methods generally promote cell-cell interactions by preventing cell-substrate interactions, thereby facilitating the rapid self-assembly of cells into multicellular aggregates. These approaches are relatively simple, offer high-throughput capabilities, and provide flexibility in combining various cell types.<sup>83</sup> Scaffold-Free 3D tumor spheroids does not require complex scaffold materials; cells naturally aggregate to form spheroids, and the culture conditions are relatively simple with a high cell density. Scaffold-Free spheroids are typically cultured in standard 96- or 384-well plates, which also means they are more suitable for high-throughput drug screening. Since tumor cells are combined in the form of spheroids, when the size of these tumor spheroids exceeds 400  $\mu\text{m}$ , they generate oxygen and nutrient gradients within the body, leading to core necrosis, a quiescent middle area, and a proliferative thick shell due to limited molecular transport. Roper et al<sup>96</sup> stained tumor spheroids using immunohistochemistry and found that hypoxia-related biomarkers (CA9) marked distinct hypoxic and non-hypoxic areas (Figure 3D), showing rapid and stable growth in three-dimensional tumor spheroids (Figure 3E), which is crucial for studying the tumor microenvironment and drug response.

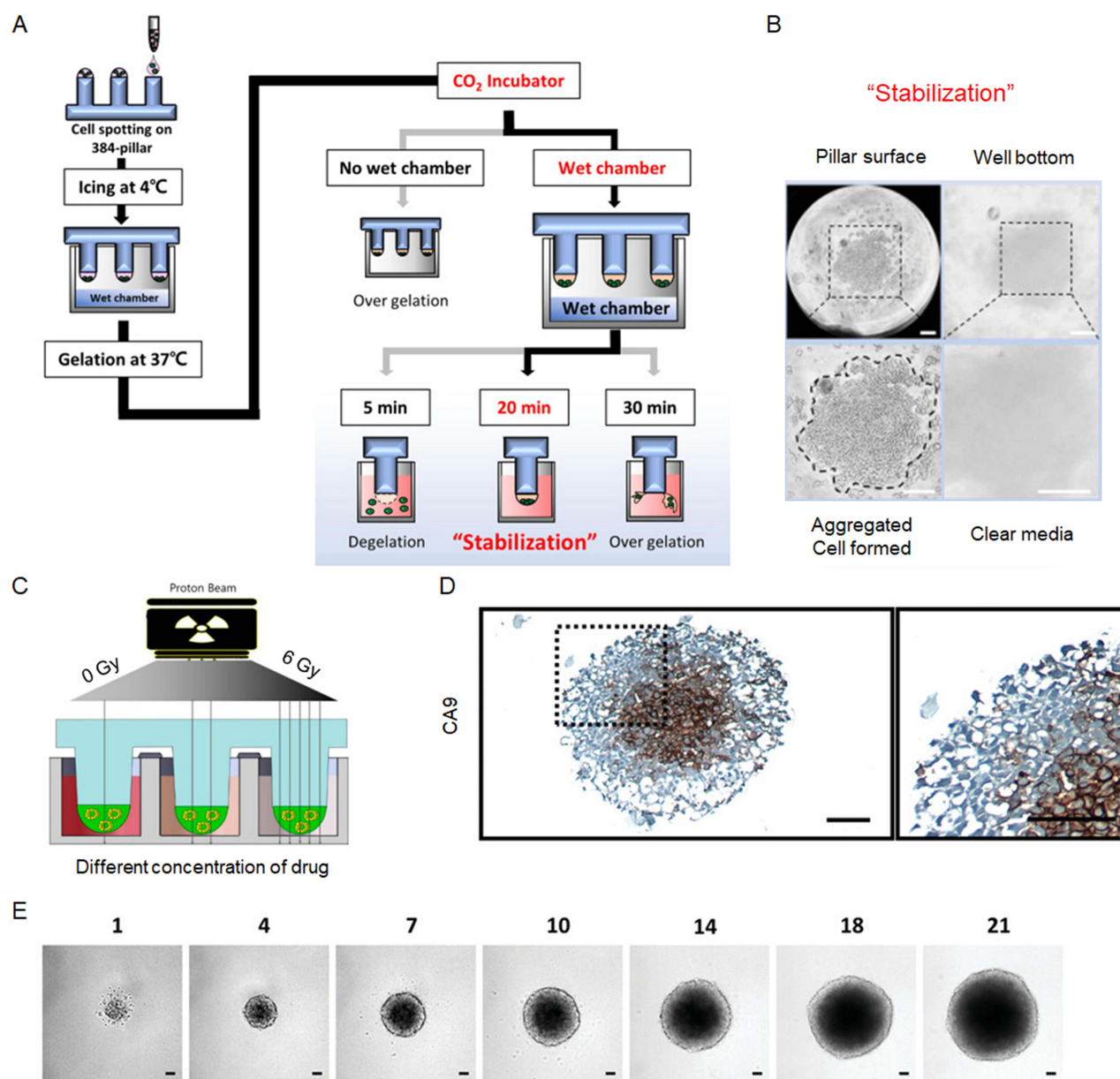


**Figure 3** Manufacturing process of 3D tumor spheroids and related experimental results. **(A)** Culture protocol for 3D cell colony spheroids for implementation of 3D-ASM. Reproduced with permission from Lee SY, Hwang HJ, Lee DW. Optimization of 3D-aggregated spheroid model (3D-ASM) for selecting high efficacy drugs. *Sci Rep.* 2022;12(1):18937. <http://creativecommons.org/licenses/by/4.0/>.<sup>97</sup> Copyright 2022, Springer Nature Ltd. **(B)** The surface of the 384 column plate and the bottom of the wet chamber. Reproduced with permission from Lee SY, Hwang HJ, Lee DW. Optimization of 3D-aggregated spheroid model (3D-ASM) for selecting high efficacy drugs. *Sci Rep.* 2022;12(1):18937. <http://creativecommons.org/licenses/by/4.0/>.<sup>97</sup> Copyright 2022, Springer Nature Ltd. **(C)** Schematic diagram of combined proton beam-drug screening. Reproduced with permission from Lee DW, Kim JE, Lee GH, et al. High-Throughput 3D Tumor Spheroid Array Platform for Evaluating Sensitivity of Proton-Drug Combinations. *Int J Mol Sci.* 2022;23(2). <http://creativecommons.org/licenses/by/4.0/>.<sup>98</sup> Copyright 2022, MDPI Ltd. **(D)** Immunohistochemical staining of hypoxic (CA9) markers of tumor spheroids at day 21 (scale:100µm). Reproduced with permission from Roper SJ, Coyle B. Establishing an In Vitro 3D Spheroid Model to Study Medulloblastoma Drug Response and Tumor Dissemination. *Curr Protoc.* 2022;2(1):e357.<sup>96</sup> Copyright 2022, Wiley-Blackwell Ltd. **(E)** Representative images of 3D tumor spheroids over a 21-day period (scale:100µm). Reproduced with permission from Roper SJ, Coyle B. Establishing an In Vitro 3D Spheroid Model to Study Medulloblastoma Drug Response and Tumor Dissemination. *Curr Protoc.* 2022;2(1):e357.<sup>96</sup> Copyright 2022, Wiley-Blackwell Ltd.

In recent years, researchers led by Li have developed a new method using hydrophobic silica nanoparticles to encapsulate liquid culture tumor spheroids and drug screening.<sup>99</sup> Compared to traditional hanging drop methods, this approach not only enables real-time in situ imaging and motion control but also more closely replicates the microenvironment of in vivo tumor tissues. However, despite some achievements in tumor spheroid culture with these traditional methods, they face challenges in constructing scalable tumor spheroid models. These methods require a large number of

cells and compounds as initial materials, which poses a barrier to applications involving rare cell-derived spheroids (eg, patient tumor biopsy samples). To overcome these limitations, researchers are exploring new strategies. One approach is to reduce the consumption of materials and cells to study spheroids from rare cells. Additionally, new methods such as using novel supporting matrices, microfluidic chip technologies are being explored to construct and control tumor spheroid models, better simulating *in vivo* physiological environments. In summary, the work of Li et al provides new insights and pathways for tumor spheroid culture, but further development and refinement are needed to better apply to the screening of rare cell-derived spheroids and personalized medicine. Researchers are committed to addressing these challenges to further advance tumor spheroid research.

In the study by Popova et al,<sup>100</sup> a platform called Droplet Microarray (DMA) was used to form highly uniform, separated, and stable nanoliter droplets on hydrophilic spots in an ultrahydrophobic background, with each droplet capturing cells to serve as a reservoir for individual biological experiments. The mentioned DMA platform significantly reduces the use of compounds, reagents, and cells, thereby reducing screening costs while increasing throughput. Several common cancer cell lines were used to construct tumor spheroids (such as MCF-7, HEK293, and HeLa cells), with tumor spheroids formed in 100 nL droplets starting from only 150 cells per droplet within 24 to 48 hours. In the study by Xia et al,<sup>101</sup> an ultrahydrophilic-ultrahydrophobic microarray platform combined with acoustic droplet technology was used. The acoustic droplet ejection device used could precisely inject drug solutions into the droplets, with the entire process completed within 20 milliseconds, achieving precise drug delivery to cell spheroids and improving the accuracy and efficiency of drug screening.

### Scaffold-Based 3D Tumor Spheroids

Scaffold-Based 3D tumor spheroids are created by utilizing natural or synthetic biomaterials, such as extracellular matrix components and hydrogels, to support cell growth and tissue formation. Tumor cells grow on a matrix that mimics the tumor cell extracellular matrix. This scaffold not only promotes cell growth but also provides essential cues from the natural biophysics and biochemical environment, which are crucial for regulating tumor cell functions.<sup>84</sup> Currently, scaffolds for *in vitro* cancer modeling have evolved from natural hydrogels (such as proteins, polysaccharides), synthetic hydrogels (such as polyethylene glycol, peptides), and hybrid materials (with high water content, tissue-like bioresponsiveness, viscoelasticity, and mechanical properties). Advances in microfabrication techniques in recent years have enabled more complex and precise hydrogel platforms, which can replicate the fundamental characteristics of the tumor microenvironment (TME). Compared to Scaffold-Free 3D tumor spheroids, these platforms offer better biocompatibility and structural stability due to the addition of scaffold materials, allowing for a more accurate simulation of the *in vivo* environment and the study of cell interactions.

Alginate, hyaluronic acid, and chitosan have been widely used to fabricate 3D tumor spheroids. For example, Sabhachandani and colleagues<sup>102</sup> used a microfluidic-based droplet platform to generate single and co-culture spheroids of breast cancer in alginate hydrogel and explored their potential for therapeutic effect screening, showing that co-culture spheroids exhibited higher drug resistance than single culture spheroids. To better mimic the natural TME, further research by the team incorporated oxygen gradient generators and immune cells into their spheroid system to study the roles of hypoxia and immune cells in spheroid growth and drug response.<sup>103,104</sup> A recent study by the team also explored the impact of immune cells on tumor response and progression.<sup>105</sup>

Matrigel is a commercially available basement membrane extract and has been the most commonly used three-dimensional cell culture matrix for constructing tumor spheroids in recent years. Matrigel's origins date back more than 40 years and are primarily composed of mouse tumor cell laminin (laminin), type IV collagen, nidogen (entactin), and heparan sulfate proteoglycan extracted from Engelbreth-Holm-Swarm (EHS) tumors. It is a complex mixture of proteins that can solidify into a gel-like state at 37°C, simulating the natural environment of the extracellular matrix (ECM).<sup>106,107</sup> Lee et al<sup>108</sup> created large uniform dense spheroids by attaching Matrigel to a 96-well plate to simulate the tumor microenvironment of hepatocellular carcinoma. Through high-throughput drug screening, the tumor model was compared with traditional 2D tumor models, showing higher drug resistance, indicating that the newly constructed 3D tumor spheroid model is closer to *in vivo* conditions. Lee et al<sup>97</sup> also used Matrigel to create an optimized 3D tumor spheroid model for drug screening. Cells and matrix gel mixtures were distributed on the surface of a 384-well plate using a 3D



cell injector. After placing the 384-well plate in a humid chamber and refrigerating for 2 hours, the cells would aggregate at one location under CO<sub>2</sub> incubator conditions. If the humid chamber and 384-well plate do not adhere properly, excessive gelation may occur. Under humid incubator and humid chamber conditions, the 3D cell mixture stabilizes after 20 minutes of gelation (5 minutes for gelation, 30 minutes for excessive gelation) (Figure 3A). In the case of a stable three-dimensional cell mixture, an aggregated cell colony can be observed on the surface of the 384-well plate, with no detached gel or free-floating cells observed at the bottom of the humid chamber (Figure 3B). Another research group<sup>98</sup> used Matrigel to construct 3D tumor spheroids on a 384-well plate to study the therapeutic effect of proton beam therapy on squamous cell carcinoma of the head and neck and observed the therapeutic effect on the spheroids by controlling the irradiation dose (Figure 3C).

Currently, cancer cells are embedded in protein-based hydrogels (such as Matrigel,<sup>109</sup> fibronectin,<sup>110</sup> and collagen<sup>111,112</sup>) to prepare various tumor spheroids. These hydrogels combine specific cell adhesion sequences and enzyme-mediated matrix degradation, which are beneficial for cell proliferation. Aisenbrey et al<sup>113</sup> discussed the limitations of Matrigel as a cell culture matrix and the applications and advantages of synthetic materials as alternatives to it in cell culture, regenerative medicine, and organoid assembly. Matrigel is a basement membrane matrix extracted from a specific type of mouse tumor, and its complex, ill-defined, and variable composition leads to uncertainty and lack of reproducibility in cell culture experiments. In the study by Kim et al,<sup>114</sup> an extracellular matrix (ECM) hydrogel derived from gastrointestinal (GI) tissue was used as an alternative to traditional Matrigel. The results demonstrated that through optimized decellularization treatment, the hydrogel retained a rich ECM component, reduced batch-to-batch variation, and improved hydrogel biocompatibility and safety.

## Organoid

Because primary tumor tissues have complex biological and clinical characteristics, their replication is limited. Tumor spheroids have been constrained in their precise prediction of individual patient responses to drugs. In contrast, organoids have overcome this limitation and are now being used as effective tools for disease modeling, drug screening, and the advancement of personalized medicine. Unlike tumor spheroids, organoids refer to cell aggregates cultured *in vitro* with a specific size and shape, capable of simulating and demonstrating partial features and functions of the corresponding tissues or organs. Typically, they are derived from stem cells or progenitor cells, and they demonstrate essential characteristics observed in native organs, such as distinctive tissue structures, gene expressions, cellular functions, and intricate multicellular features.<sup>85–87</sup> Importantly, tumor organoids retain the key structural and functional features of their *in vivo* counterparts, potentially providing an unprecedented predictive relevant *in vitro* platform for clinical decision-making.

Tumor organoids are typically generated in gels made from Matrigel, which is the “gold standard” hydrogel for 3D culture. The main components include four major basement membrane proteins: approximately 60% laminin, about 30% type IV collagen, about 8% entactin, and 2–3% heparan sulfate proteoglycan.<sup>115</sup> Despite their proven applicability, the presence of immunogenicity and batch-to-batch variability continues to trouble researchers, reducing the reliability of Matrigel as a matrix source for patient-derived organoid (PDO) model culture. Due to the limitations of matrix gels in terms of physical and biochemical manipulation, adjusting the matrix to promote specific cell behaviors and achieve desired biological outcomes is challenging.<sup>113</sup> Biomimetic hydrogels, including proteins, polysaccharides, and synthetic hydrogels, have emerged as excellent alternatives to matrix gels. Ng et al<sup>116</sup> demonstrated that enzymatically crosslinked gelatin, which has the ability to independently modulate stiffness and composition, can support the growth and metabolism of colorectal cancer organoids compared to cells cultured in Geltrex.

In a static three-dimensional culture, organoids mainly depend on passive diffusion to enable the transfer of nutrients and removal of waste. However, as the organoids grow and mature, diffusion transport becomes insufficient to meet their demands. To overcome this challenge, organoid chip platforms combining microfluidic technology have become one of the solutions.<sup>117</sup> This platform has the capability to dynamically provide nutrients under physiological flow conditions, supporting the growth and development of organoids. An example is the lung cancer chip platform developed by Jung et al, which includes 29 microchambers and a flow microchannel. This platform is used for cultivating and conducting drug sensitivity testing on primary lung PDOs under continuous flow conditions.<sup>118</sup> In comparison to static culture

conditions, the three-dimensional lung cancer organoids showed increased sensitivity to cisplatin and etoposide in the microfluidic platform, attributed to improved drug permeability. This platform effectively preserves the patient's original tumor morphology and genetic characteristics. These results indicate that the platform can provide a more physiologically relevant three-dimensional tumor environment for predicting drug responses.

In another research, Shirure et al created a vascularized tumor organoid to replicate the pathological flow conditions within blood vessels.<sup>119</sup> By co-culturing tumor organoids and perfused three-dimensional microvascular networks in a five-channel microfluidic device, this model can replicate the realistic *in vivo* vascular supply and transport characteristics. These vascularized organoids can be maintained under physiologic flow for 22 days. The study also demonstrated a significant reduction in tumor proliferation after paclitaxel vascular perfusion, showing the potential to assess individual responses to chemotherapy in clinical trials, based on the specific patients.

In summary, the organoid chip platform combined with microfluidic technology can overcome the challenges of nutrient supply faced by organoids under static culture conditions. These systems offer a more relevant physiological setting for simulating drug reactions and assessing treatment approaches for diseases. Furthermore, vascularized organoid chips can also mimic *in vivo* vascular supply and transport characteristics, providing a more realistic model for studying tumor development and drug efficacy.

Organoids play a crucial role in the field of tissue engineering and regenerative medicine research, offering a more realistic *in vitro* model that closely resembles the structure and function of human organs. By regulating culture conditions, organoids can be developed with specific cell types and tissue structures, allowing them to simulate particular physiological or pathological processes.<sup>120</sup> Excellent tools like organoids have been utilized for disease modeling, drug screening, and the advancement of personalized medicine. Over the last decade, there has been significant advancement in creating a variety of human organoids, including the brain,<sup>121,122</sup> kidney,<sup>123,124</sup> retina,<sup>125</sup> lung,<sup>126,127</sup> prostate,<sup>128</sup> liver,<sup>129,130</sup> and gastrointestinal tissues.<sup>131–133</sup> The use of tumor organoids enables drug screening and the investigation of tumor development processes. Therefore, this multifaceted technology is considered the next generation of tumor models, promoting the development of various novel human tumor models.

In the context of breast cancer, Sachs aimed to effectively generate representative and robust BC models to supplement molecular and pathological breast cancer-related analyses. In their work, Sachs et al<sup>134</sup> detailed a method for the extended cultivation of human breast epithelial organoids. This led to the development of over 100 primary and metastatic breast cancer organoid lines that broadly mirror the diversity of the disease. The success rate of establishing breast cancer organoids has been improved to over 80%. The morphology of breast cancer organoids aligns with the histopathology, hormone receptor status, and HER2 status of the original tumors. No deviation in histological subtypes, grading, or receptor status compared to the original breast cancer was observed. Camilla Calandrini and colleagues<sup>135</sup> have established the first organoid biobank for pediatric kidney cancers, deriving tumor and matched normal kidney organoids from over 50 children with various subtypes of renal cancers. This includes Wilms tumors, malignant rhabdoid tumors, renal cell carcinomas, and congenital mesoblastic nephromas. These pediatric kidney tumor organoids retain key characteristics of the original tumors, which is highly beneficial for uncovering patient-specific drug sensitivities. The research team has conducted histological characterization of the pediatric renal cancer organoids, indicating that the tumor organoids closely resemble their parent tumor tissues. Furthermore, the triphasic nature of Wilms tumors, comprising epithelial, stromal, and blastemal components, appears to be preserved in organoid cultures (Figure 4A). Schuth et al<sup>136</sup> conducted research on the role of cancer-associated fibroblasts (CAFs) in pancreatic ductal adenocarcinoma (PDAC) progression and chemoresistance. They established direct three-dimensional co-cultures of primary PDAC organoids and patient-matched CAFs to confirm the impact of CAFs on sensitivity to gemcitabine, 5-fluorouracil, and paclitaxel treatment. The results, demonstrated in Figure 4B and C, revealed increased proliferation and reduced chemotherapy-induced cell death of PDAC organoids when co-cultured with CAFs. This underscores the potential of personalized PDAC co-culture models for not only drug response analysis but also for elucidating the molecular mechanisms of tumor stroma chemotherapy resistance support.

Using primary mouse and human induced pluripotent stem cell-derived lung epithelial cells, Dost et al<sup>137,138</sup> created organoid systems to mimic early-stage lung adenocarcinoma. Their aim was to investigate the molecular changes occurring shortly after the activation of the oncogenic KRAS gene in lung epithelial cells. Additionally, van de



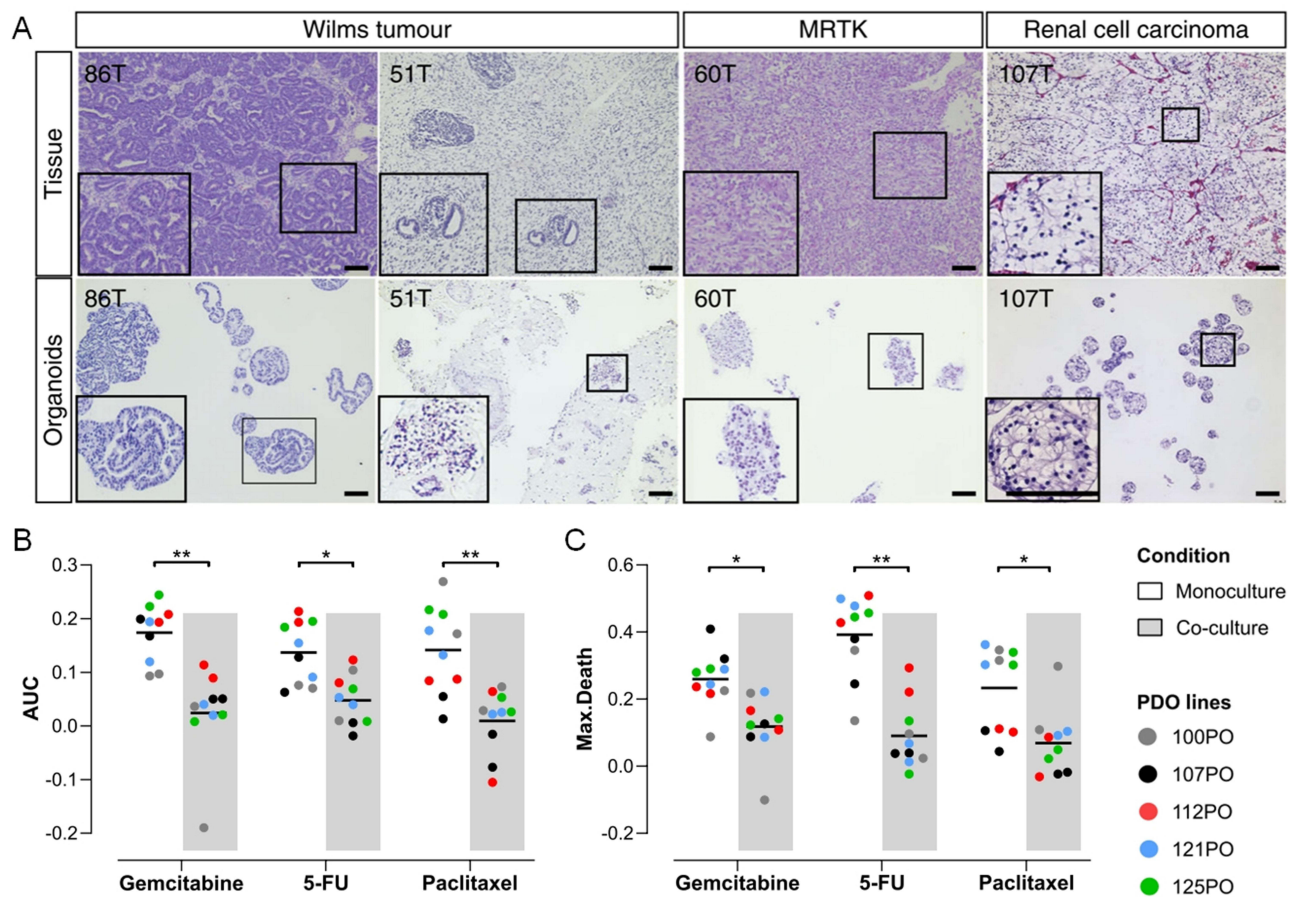


**Figure 4** Organoids can retain the properties of tumors very well. **(A)** H&E staining on tissue (top) and matching organoids (bottom) derived from the indicated tumour types ( $n = 3$ ). Scale bars: 100  $\mu\text{m}$ , zoom in 50  $\mu\text{m}$ . Reproduced with permission from Calandrini C, Schutgens F, Oka R, et al. An organoid biobank for childhood kidney cancers that captures disease and tissue heterogeneity. *Nat Commun.* 2020;11(1):1310. <http://creativecommons.org/licenses/by/4.0/>.<sup>135</sup> Copyright 2020, Springer Nature. **(B) (C)** When co-cultured with CAF, the PDAC organoids exhibited a significant reduction in cell death induced by gemcitabine, 5-FU, and paclitaxel, as indicated by the mean of two independent repeat assays per line. This was confirmed by the paired *T*-test, where \*  $P < 0.05$  and \*\*  $P < 0.01$ . Reproduced with permission from Schuth S, Le Blanc S, Krieger TG, et al. Patient-specific modeling of stroma-mediated chemoresistance of pancreatic cancer using a three-dimensional organoid-fibroblast co-culture system. *J Exp Clin Cancer Res.* 2022;41(1):312. <http://creativecommons.org/licenses/by/4.0/>.<sup>136</sup> Copyright 2022, BioMed Central Ltd.

Wetering et al<sup>139</sup> reported the development of tumor organoid cultures from 20 consecutive colorectal cancer (CRC) patients, where they identified abnormal Wnt signaling pathway mutations. Furthermore, they observed variations in the number of primary tumor organoids among patient samples, ranging from thousands in some tumors to only 10–20 in others. This derived difference may reflect the heterogeneous composition of the tumors. Additionally, successful construction of various other tumor organoids<sup>140–142</sup> has been documented, fully demonstrating the role of organoid technology in bridging the gap between cancer genetics and patient trials, supplementing drug research based on cell lines and xenografts, and promoting personalized treatment design.

Organoids offer a novel platform for personalized medicine and drug development. They enable the evaluation of drug effectiveness and potential side effects based on individual conditions. These structures can reproduce the structural and functional traits of the tumor microenvironment (TME) and are considered advanced 3D in vitro models for drug testing and fundamental cancer biology research. Currently, human clinical trials have commenced incorporating organoids for drug screening.<sup>143</sup> Yet, there are still challenges that must be overcome to streamline this process. One such challenge involves refining the culture conditions necessary for generating organoids to improve their growth, development, and stability. Additionally, efforts are required to minimize the time and cost of organoid culture, thereby expanding their applications in the fields of medicine and drug development. Another challenge is how to incorporate stromal cells, especially immune cells, to better reflect the cell interactions and immune responses in the tumor

microenvironment. By overcoming these challenges, organoids can provide more accurate and reliable predictive models for personalized medicine and drug development, aiding in the selection of the most effective treatment and reducing the failure rate in the drug development process. Through the utilization of organoids, we can enhance our comprehension of the intricacies of diseases and establish a strong basis for precision medicine.

## Tumor Chip

Statistics show that approximately 90% of cancer-related deaths are caused by tumor metastasis. Our knowledge of the potential cellular and molecular mechanisms propelling the metastatic process remains limited, and traditional models face challenges in fully reproducing this highly intricate process.<sup>88,89</sup> Consequently, numerous microfluidic models have been created to investigate the cellular and molecular functions involved in the series of tumor metastasis, which is crucial for uncovering therapeutic intervention opportunities in early metastatic spread. The tumor chip, a miniature experimental platform, is used to simulate and study the biological characteristics and treatment responses of tumors. By arranging tumor-related cells, tissues, or molecules on a chip, it can simulate the complex and diverse tumor environment *in vitro*. The tumor chip, typically consisting of microfluidics and microstructures, has the ability to mimic and control the interactions between cells within the tumor and between cells and the stroma, providing a reliable biological environment for studying tumor growth, metastasis, drug resistance, and development processes.

In recent decades, the development of microfluidic technology and bioprinting has led to the emergence of water-based hydrogel microfluidic platforms. These systems replicate crucial elements of the tumor microenvironment, like the cascade of cancer metastasis, dynamic blood flow, interactions between cells and the stroma, and have the capability to predict patient responses accurately. Thus, they are positioned to replace conventional experimental models as they can precisely control various microenvironmental factors and combine different cell types *in vitro*. Moreover, due to the lower cell quantities required for microfluidic models compared to traditional patient biopsy samples, they offer distinct advantages. By creating cancer metastasis cascade models on chips, we can study angiogenesis, tumor cell invasion, and simulate the intravasation and extravasation of tumor cells. Microfluidic platforms can be used for cancer drug screening and the development of personalized cancer treatment. Tumor chips serve as a dependable research platform, enhancing our comprehension of the intricate process of tumor metastasis and presenting fresh opportunities for early intervention in metastatic spread.

Additionally, the exceptional regulation of fluid flow makes vascularized tumor chips particularly useful for studying how tumors respond to medications under natural blood flow conditions. Angiogenesis plays a crucial role in cancer progression, signifying the shift from tumor growth to advancement,<sup>90</sup> making it a key factor in managing cancer growth and advancement. Various microfluidic devices based on water-based hydrogels have been created to assess the role of tumor cells in promoting angiogenesis. Furthermore, angiogenic factors (such as VEGF, HGF,  $\beta$ -FGF, etc.) can stimulate the development of vascular sprouts.<sup>144–146</sup> Research by Nguyen et al demonstrated an organotypic microfluidic platform that reproduced the formation of vascular sprouts and new microvessels using engineered vessels in a collagen matrix.<sup>144</sup> Through this model, researchers observed the invasion of capillary sprouts and their connection to the surrounding stroma, eventually integrating with functional new vessels upon perfusion of nearby lumens with angiogenic factors. Vascularized tumor chips are particularly suitable for studying the response of tumors to drugs under physiological blood flow conditions. The progression of cancer is significantly influenced by angiogenesis, and water-based hydrogel microfluidic devices can help us understand the mechanisms of tumor cell-induced angiogenesis and achieve valuable results in simulating the formation of vascular sprouts and new microvessels.

To achieve metastasis, cancer cells must first degrade the surrounding extracellular matrix (ECM) and then penetrate the matrix. Throughout this process, cancer cells interact and communicate with all elements within the tumor microenvironment (TME) that affect the outcome of metastasis, including endothelial cells, stromal cells, immune cells, hypoxia, chemokines, and ECM components.<sup>147</sup> For instance, factors secreted by tumor cells induce the differentiation of stromal cells into cancer-associated fibroblasts (CAFs), which, as the primary depositors of the ECM, support tumor growth by secreting various ECM components and enzymes, such as transforming growth factor-beta (TGF- $\beta$ ) and platelet-derived growth factor (PDGF).<sup>148,149</sup> Additionally, endothelial cells promote the adhesion

and extravasation of tumor cells by secreting ECM components like fibronectin.<sup>150</sup> Immune cells, particularly macrophages and neutrophils, participate in ECM remodeling by secreting ECM-degrading enzymes, such as matrix metalloproteinases (MMPs), thereby influencing tumor invasion and metastasis.<sup>151</sup> These findings reveal the critical role of ECM remodeling in cancer development and metastasis and provide potential targets for the development of novel therapeutic strategies targeting the ECM remodeling process. For example, drugs targeting specific ECM components or their receptors could be designed to block or alter signaling pathways that promote cancer progression. Moreover, modulating the physical properties of the ECM, such as its stiffness or architecture, may help inhibit cancer cell invasion and metastasis.

Microfluidic technology has been widely applied to elucidate the functions of different types of cells in tumor cell migration and invasion. In one study, researchers used a microfluidic device combined with a 3D hydrogel matrix to detect the paracrine interactions between human SUM159 breast cancer cells and patient-derived tumor-associated fibroblasts (CAFs).<sup>152</sup> By inducing the expression of the non-metastatic glycoprotein B (GPNMB) in breast cancer cells, CAFs significantly increased the migration speed of breast tumor cells in the three-dimensional matrix. In addition to stromal cells, endothelial cells and immune cells also influence the invasive ability of cancer cells. Nagaraju and colleagues designed a microfluidic device with three layers to facilitate the co-culturing of MDA-MB-231 breast cancer cells and HUVECs endothelial cells in separate channels. The device allows for the interaction between the two cell types under controlled conditions. The results showed enhanced invasiveness of tumor cells in association with spontaneously formed vessels. Additionally, the blood vessels formed in the presence of tumor cells exhibited greater permeability and were thinner when compared to *in vivo* studies.<sup>153</sup> Nguyen and colleagues<sup>154</sup> established a chip model for pancreatic ductal adenocarcinoma (PDAC) to validate the invasive nature of PDAC cells (PD7591 cell line) into the vascular lumen., where they disintegrate endothelial cells, leaving behind a tumor-filled lumen structure. The microfluidic device comprises a matrix with two hollow cylindrical channels. One channel is seeded with human umbilical vein endothelial cells (HUVEC) to create a perfusable biomimetic vessel, while the other is seeded with pancreatic cancer cells to form a pancreatic ductal adenocarcinoma (Figure 5A). This model replicates vascular invasion and tumor-vascular interactions, offering insight into PDAC-vascular interactions. The findings indicated that the presence of HUVEC increased the migration speed of PD7591 (Figure 5B), demonstrating the model's effectiveness. In later stages of the experiment, PD7591 cells were observed invading around the vessels and inducing apoptosis of the human umbilical vein endothelial cells (Figure 5C).

The invasive abilities of cancer cells are also influenced by the biochemical and biophysical signals present in the tumor microenvironment (TME). By integrating three-dimensional hydrogels into microfluidic platforms, stable chemical gradients can be established for studying three-dimensional invasion trends. In their study, researchers created oxygen gradients using chemical gradients to explore the effects of hypoxia on cancer cell migration in a three-dimensional culture.<sup>155</sup> Microfluidic technology has been extensively utilized to investigate the roles of different cell types in cancer cell migration and invasion. Through the integration of 3D hydrogel matrices and the establishment of chemical gradients, microfluidic platforms offer a robust approach to studying the impact of various factors in the tumor microenvironment on cancer cell invasion.

## Vascularization of Tumor Models

When tumor cells grow rapidly, their demand for oxygen and nutrients also increases. The rapid growth of tumor tissue leads to insufficient blood supply, causing a lack of adequate oxygen and resulting in hypoxia, which is a significant hallmark of the tumor microenvironment.<sup>156</sup> Hypoxia is present in almost all cancers, defined as areas with oxygen levels below 2%. The rapid growth of tumor cells and the resulting mismatched oxygen supply lead to this imbalance. Hypoxia in turn can induce various biological changes in cancer cells, including modifications in gene expression and metabolism, fostering increased aggressiveness and resistance to chemotherapy.<sup>157</sup>

The growth and spread of cancer rely on the essential role of the vascular system connected to endothelial cells in delivering oxygen and nutrients.<sup>158</sup> Hypoxic signals activate the expression of vascular endothelial growth factor (VEGF) and other angiogenic factors, stimulating the formation of new blood vessels through molecular pathways.<sup>159</sup> This process, referred to as angiogenesis, is a critical feature of cancer. With the assistance of new blood vessels, tumors can



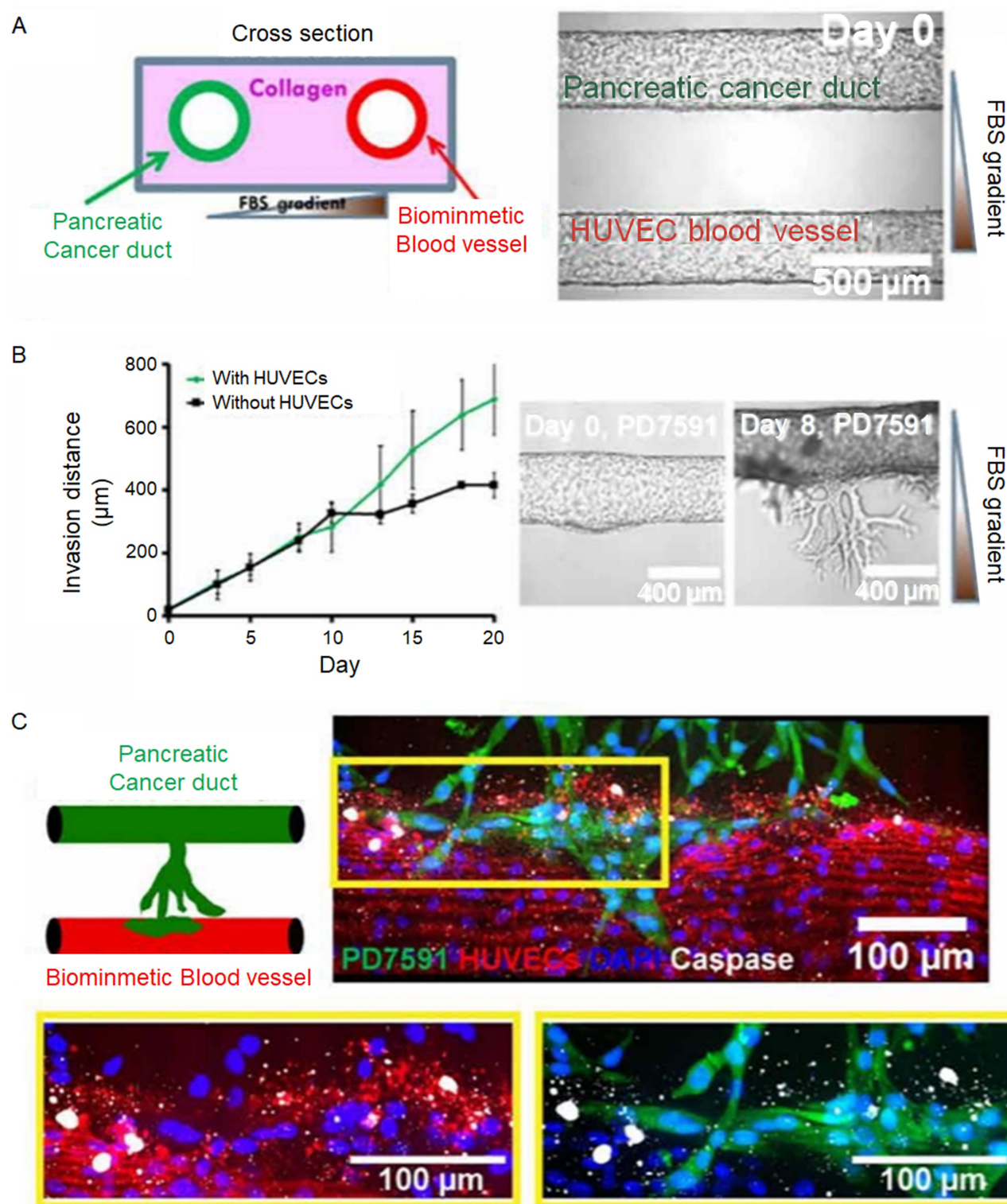


**Figure 5** Organotype model of vascular invasion of pancreatic tumors captured by PDAC chips. **(A)** Illustration of a PDAC chip featuring artificial blood vessels and pancreatic cancer ducts, along with phase-contrast images displaying the implanted cells in the device prior to PDAC migration. **(B)** The average invasion distance of PDAC cell line PD7591 in response to FBS gradients of human umbilical vein endothelial cells (HUVEC) with and without human umbilical vein endothelial cells. Exemplar phase-contrast images of PD 7591 migration on days 0 and 8 exhibit the collective migration of PDAC invasion. **(C)** Within the model, endothelial cell apoptosis (marked in red and highlighted by lysed caspase 3 staining in white) was observed during the vascular invasion of PD 7591 (shown in green). Endothelial cells in all images were stained with anti-CD31 antibodies. PD 7591 was re-stained with FITC-conjugated anti-GFP (green fluorescent protein) antibody. The nucleus is stained with 4', 6-diamidino - 2-phenylindole (DAPI) (in blue). Reproduced with permission from Nguyen DT, Lee E, Alimperti S, et al. A biomimetic pancreatic cancer on-chip reveals endothelial ablation via ALK7 signaling. *Sci Adv.* 2019;5(8):eaav6789.<sup>154</sup> Copyright 2019, American Association for the Advancement of Science Ltd.

expand to a diameter of 2–3 millimeters or larger.<sup>160</sup> For instance, under hypoxic conditions, the accumulation of HIF protein occurs due to the inability of the tumor suppressor protein to degrade, as HIF-1 has been identified as a key regulator in mammalian cell response to hypoxia. In recent years, there has been significant interest in treatments targeting HIF-1.<sup>161</sup> These factors contribute to the dispersion and migration of endothelial cells, ultimately leading to the formation of new vascular structures. These newly formed blood vessels can supply the necessary oxygen and nutrients to the tumor tissue, aiding in its continued growth and proliferation.

Blood vessels are the cornerstone of survival for nearly all functional tissues. These perfusable networks function to carry nutrients, oxygen, and bioactive substances to various organs or locations within the tissue, while also eliminating metabolic waste products like acids and carbon dioxide, aiming to uphold the body's internal environment equilibrium.<sup>162,163</sup> Without an interconnected network of blood vessels, tissues cannot survive independently. However, compared to the normal vascular system, the tumor vascular system displays abnormal morphological and functional characteristics, such as irregular vessel networks, leakage, and uneven blood flow. These alterations in the vascular network result in heightened interstitial fluid pressure (IFP) and hypoxic regions, ultimately supporting tumor survival and metastasis.<sup>164,165</sup> Additionally, the abnormal vascular system also restricts the impact of new immune cells and anti-cancer therapies on the tumor, ultimately reducing the effectiveness of cancer treatment.<sup>166</sup> Therefore, simulating the vascular system in tumor models is crucial and necessary.

In the production of tumor models, *in vitro* conditions, such as in perfused bioreactors, can provide a vascular structure for the supply of oxygen and nutrients. However, once implanted in the body, the delivery of oxygen and nutrients is often restricted by diffusion kinetics. Due to the relatively slow rate of oxygen diffusion in tissue compared to consumption, oxygen becomes a crucial factor limiting cell survival. Therefore, when tissue thickness surpasses the limit of nutrient diffusion, the need for vascularization becomes paramount, particularly for tissues with high oxygen consumption rates, such as the heart, pancreas, and liver tissues. Most cells cannot tolerate distances from blood vessels exceeding 200  $\mu\text{m}$ , and sensitive cells like islets may experience reduced activity or even necrosis if the oxygen diffusion distance exceeds 100  $\mu\text{m}$ . Conversely, cartilage cells typically exhibit greater resistance and can remain viable in transplants with a thickness exceeding 1mm.<sup>167</sup> Hence, the construction of tumor models requires the integration of multi-scale vascular, lymphatic, and/or neural networks.

To overcome current limitations, two primary approaches have been designed: First, by patterning growth factors or cells within the tissue structure to promote vascular development. Vascular endothelial growth factor (VEGF) is a short-lived substance that effectively promotes angiogenesis. In both *in vivo* and *in vitro* experiments, controlled release of VEGF within gelatin microspheres (GMP) has been proven to facilitate long-term vascularization.<sup>168</sup> Due to the high specificity of the vascular system produced by this method, it is difficult to replicate on a one-to-one basis, leading us to favor the second approach. Another method is to integrate microchannels without vasculature to enhance the diffusion of oxygen and nutrients. Studies have shown that integrating microchannels into tissue structures can help nutrients diffuse towards printed cells, effectively addressing the 200  $\mu\text{m}$  diffusion limitation for cell survival in engineered tissues.<sup>169</sup> Bertassoni et al<sup>170</sup> demonstrated the formation of fully permeable microchannels by printing agarose at specific locations, encapsulating printed cells with methacrylated gelatin (GelMA) hydrogel, and then removing the template from the surrounding photocrosslinked gel after gelation. The effectiveness of this method in achieving the desired microchannel effect can be observed through contrast images of green fluorescent bioprinted templates and pink fluorescent suspensions. Cell viability assays also show that cells within gels containing microchannels exhibit higher activity. This method is typically applicable to complex tumor models with three-dimensional structures, such as 3D tumor spheroids and organoids. Due to the insufficient strength of hydrogels to maintain long-term tubular structures under pressure, to address this issue, Gu et al<sup>171</sup> introduced a strategy based on 3D printing technology for constructing nanofibrous poly (L-lactide)/poly( $\epsilon$ -caprolactone) (PLLA/PCL) scaffolds with interconnected perfusable microchannel networks (IPMs). These scaffolds are designed to simulate the engineering requirements of vascularized bone tissue, achieving customized microchannel patterns through a combination of phase separation and sacrificial template methods. The study investigated the impact of microchannel structure on angiogenesis and osteogenesis, finding that 0.5/0.8-IPMs and 0.5/1-IPMs scaffolds (with spacing to diameter ratios of 0.5/0.8 and 0.5/1, respectively) performed better in vascular network formation compared to other groups. Additionally, migration and scratch assays revealed that the VEGF@IPMs-0.5/0.8



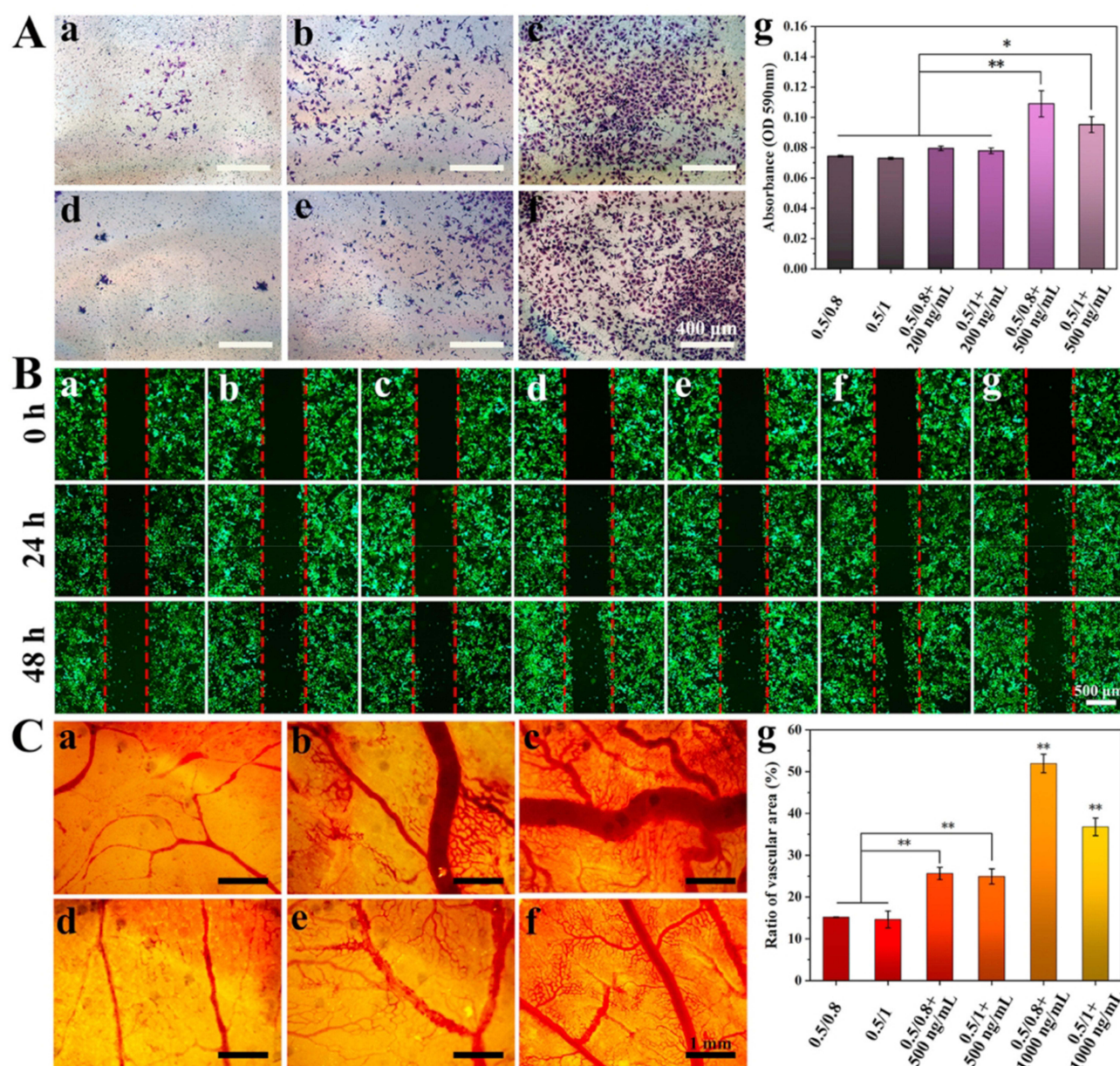


**Figure 6** The migration effects of HUVECs and the pro-angiogenesis effects of different samples in the CAM model. **(A)** The effects on HUVECs migration in the Transwell assay. **(A-a, A-b, A-c)** are all 0.5/0.8 hydrogels, the VEGF concentration is 0, 200, and 500 ng/mL, respectively. **(A-d, A-e, A-f)** are all 0.5/1 hydrogels, the VEGF concentration is 0, 200 and 500 ng/mL. **(A-g)** Quantification of the Transwell assay. **(B)** The effects on HUVECs migration in the scratch wound assay. **(B-a)** control, **(B-b, B-c, B-d, B-e, B-f)** are all 0.5/0.8 hydrogels, the VEGF concentration is 0, 200 and 500 ng/mL. **(B-g)** are all 0.5/1 hydrogels, the VEGF concentration is 0, 200 and 500 ng/mL. **(C)** Optical images of neo-blood vessel formation after 48 h of treatment with different samples in the CAM model. **(C-a, C-b, C-c)** are all 0.5/0.8 hydrogels, the VEGF concentration is 0, 500 and 1000 ng/mL. **(C-d, C-e, C-f)** are all 0.5/1 hydrogels, the VEGF concentration is 0, 500 and 1000 ng/mL. **(C-g)** The percentage of vascular area. \* $P < 0.05$ , \*\* $P < 0.01$ . Reproduced with permission from Gu J, Zhang Q, Geng M, et al. Construction of nanofibrous scaffolds with interconnected perfusable microchannel networks for engineering of vascularized bone tissue. *Bioact Mater.* 2021;6(10):3254–3268. <https://creativecommons.org/licenses/by-nc-nd/4.0/>.<sup>171</sup> Copyright 2021, KeAi Communications Co.

scaffold demonstrated superior effects in promoting the migration of human umbilical vein endothelial cells (HUVECs) and neo-vascularization (Figures 6A-C). Experiments on the expression of osteogenic genes RUNX2, OCN, OPN, and Col I confirmed that the VEGF@0.5/0.8 IPMs scaffold group had higher mRNA expression levels of these osteogenic markers, indicating a stronger osteogenic effect.



## Conclusions and Future Perspective

The field of 3D bioprinting has undergone rapid advancement in recent years, progressing from initial printing solely for concept validation to the current capability of printing complex multi-tissue structures. 3D bioprinting technology has demonstrated significant potential for organ transplantation and tissue reconstruction, such as for nerves and cartilage. While significant progress has been made in the field of bioprinting, a current trend involves the development of systems capable of integrating multiple materials into a single structure with diverse mechanical properties and cellular compositions, as well as producing hollow and perfusable vascularized structures. Nevertheless, a prevalent limitation of existing bioprinting systems is the prolonged manufacturing time for complex biomimetic tissues, primarily due to slow bioprinting speed. This can sometimes exceed the available time limits for creating large bioprinted tissues. Particularly in cases where switching between different materials or achieving very high bioprinting resolution is required, the time needed to manufacture functional structures significantly increases. Even though efforts have been directed towards reducing manufacturing time, such as employing a single nozzle to extrude multiple materials in bioprinting, the overall speed remains inadequate for the rapid production of customized tissues, posing a future challenge that needs to be tackled.<sup>172</sup> Various 3D bioprinting technologies have been created, each possessing its own set of pros and cons., such as high precision in inkjet printing but difficulty in forming complex 3D structures, and good three-dimensional forming capabilities but needing improvement in precision for micro-extrusion printing. In general, there is a need for bioprinters to continue enhancing printing precision and speed, while also offering additional functionalities such as multi-nozzle or multi-channel printing, automatic height adjustment, and intelligent process optimization. Managing heterogeneous components within the three-dimensional structure represents a key focus for the advancement of bioprinting technology.<sup>173</sup>

Furthermore, to better mimic the extracellular matrix environment of tissues and organs *in vivo* and achieve the corresponding functional and mechanical requirements, bioink materials generally should have certain material component combinations or gradient distributions.<sup>174</sup> In addition, there is also a future emphasis on the development of specialized inks for specific applications. To adapt to the printing process, bioink materials often require targeted modification or component design. In addition to using single or known-component inks, future developments may involve the use of decellularized extracellular matrix (dECM) materials for printing, which are directly obtained from animal tissues after decellularization processing and contain all the material factors required for tissue formation and maturation.<sup>71</sup> Through the analysis of the composition and structure of dECM, the selection and matching of inks can be better guided. Scientists are dedicated to developing dECM with the ability to induce organ-specific cellular behaviors with high cell viability, activity, and inducing organ-specific behaviors for organ replication. Many different types of bioinks have been extensively studied for manufacturing biomimetic tissues, and new bioinks are continually being developed to improve the biological similarity of bioprinted structures. However, although these bioinks can induce certain organ-like behaviors in cells, they often still represent a “synthetic” environment and are challenging to completely mimic the actual composition of organ-specific ECM. To address this issue, a promising solution is the use of decellularized ECM (dECM), as it can completely simulate the complex environmental composition of real tissues; however, the process of extraction, purification, and modification of the matrix is time-consuming, and the quantity of obtainable bioinks is limited.<sup>175</sup> However, dECM remains a highly promising source of bioinks, offering the potential to accurately replicate the intricate environmental composition of real tissues. Further research could expand the use of dECM in bioprinting.

To creatively address this challenge, one approach is to utilize decellularized extracellular matrix (dECM) extracted from patient tumors.<sup>176,177</sup> It is worth noting that during tumor progression, the mechanical stiffness of the surrounding extracellular matrix continuously increases. It has been demonstrated that the increase in matrix stiffness is associated with tumor proliferation and chemoresistance.<sup>178</sup> The discovery of the compelling mechanical characteristic of stress relaxation<sup>179</sup> has recently been shown to impact cell behavior and drug reactions. As a result, the supportive matrix for 3D culture should replicate the biochemical and physical cues of the original tumor microenvironment. In summary, research on bioinks is progressing towards mimicking the native tissue properties more closely, with dECM serving as a promising source of bioink that can provide a more realistic tissue environment. Future research will further drive the development of bioprinting technology, offering more possibilities for the manufacturing of customized tissues.

Due to the significant heterogeneity among and within patients, leading to considerable variations in their response to cancer treatment, developing in vitro models using patient-derived cancer cells is necessary to replicate the tumor microenvironment (TME), with cells sourced from patients or induced pluripotent stem cells (iPSCs) being potential options. However, creating such models is challenging due to the specific isolation protocols and culture conditions required to maintain the functionality of different cell types. Recent research on breast cancer has demonstrated that optimizing the culture medium can enhance this situation.<sup>134</sup> However, it is currently unclear whether this approach is applicable to other types of cancer, and the efficiency of tumor-like formation.<sup>180</sup>

Furthermore, a newly emerging concept, 4D Bioprinting, may also be a significant future development direction.<sup>181</sup> It adds a time dimension on the basis of 3D printing, with the most common example being the printing of shape memory materials: after the three-dimensional cell-containing structure is formed, the entire or local structure undergoes shape deformation through the stimulation of environmental factors or spontaneous initiation. Under the influence of certain stimulating factors, this deformation exhibits reversible and controllable characteristics. 4D bioprinting is expected to demonstrate great potential in regulating cell behavior, vascular formation, and tissue maturation.<sup>182</sup>

## Disclosure

The authors report no conflicts of interest in this work.

## References

1. Sung H, Ferlay J, Siegel RL, et al. Global Cancer Statistics 2020: GLOBOCAN Estimates of Incidence and Mortality Worldwide for 36 Cancers in 185 Countries. *CA Cancer J Clin.* 2021;71(3):209–249.
2. Wong CH, Siah KW, Lo AW. Estimation of clinical trial success rates and related parameters. *Biostatistics.* 2019;20(2):273–286.
3. Malda J, Visser J, Melchels FP, et al. 25th anniversary article: engineering hydrogels for biofabrication. *Adv Mater.* 2013;25(36):5011–5028.
4. Tasoglu S, Demirci U. Bioprinting for stem cell research. *Trends Biotechnol.* 2013;31(1):10–19.
5. Ren X, Ott HC. On the road to bioartificial organs. *Pflugers Arch.* 2014;466(10):1847–1857.
6. Fang Y, Frampton JP, Raghavan S, et al. Rapid generation of multiplexed cell cocultures using acoustic droplet ejection followed by aqueous two-phase exclusion patterning. *Tissue Eng Part C Methods.* 2012;18(9):647–657.
7. Jentsch S, Nasehi R, Kuckelkorn C, Gundert B, Aveic S, Fischer H. Multiscale 3D Bioprinting by Nozzle-Free Acoustic Droplet Ejection. *Small Methods.* 2021;5(6):e2000971.
8. Arnold CB, Brown MS, Kattamis NT. Finite element analysis of blister formation in laser-induced forward transfer. *J Mater Res.* 2011;26(18):2438–2449.
9. Mandrycky C, Wang Z, Kim K, Kim DH. 3D bioprinting for engineering complex tissues. *Biotechnol Adv.* 2016;34(4):422–434.
10. Chang R, Nam J, Sun W. Effects of dispensing pressure and nozzle diameter on cell survival from solid freeform fabrication-based direct cell writing. *Tissue Eng Part A.* 2008;14(1):41–48.
11. Nair K, Gandhi M, Khalil S, et al. Characterization of cell viability during bioprinting processes. *Biotechnol J.* 2009;4(8):1168–1177.
12. Hribar KC, Choi YS, Ondeck M, Engler AJ, Chen S. Digital Plasmonic Patterning for Localized Tuning of Hydrogel Stiffness. *Adv Funct Mater.* 2014;24(31):4922–4926.
13. Kadry H, Wadnap S, Xu C, Ahsan F. Digital light processing (DLP) 3D-printing technology and photoreactive polymers in fabrication of modified-release tablets. *Eur J Pharm Sci.* 2019;135:60–67.
14. Ma Y, Wei W, Gong L, et al. Biomacromolecule-based agent for high-precision light-based 3D hydrogel bioprinting. *Cell Rep Phys Sci.* 2022;3(8):100985.
15. Mironov V, Boland T, Trusk T, Forgacs G, Markwald RR. Organ printing: computer-aided jet-based 3D tissue engineering. *Trends Biotechnol.* 2003;21(4):157–161.
16. Barron JA, Wu P, Ladouceur HD, Ringeisen BR. Biological laser printing: a novel technique for creating heterogeneous 3-dimensional cell patterns. *Biomed Microdevices.* 2004;6(2):139–147.
17. Moon S, Hasan SK, Song YS, et al. Layer by layer three-dimensional tissue epitaxy by cell-laden hydrogel droplets. *Tissue Eng Part C Methods.* 2010;16(1):157–166.
18. Wilson WC Jr, Boland T. Cell and organ printing 1: protein and cell printers. *Anat Rec a Discov Mol Cell Evol Biol.* 2003;272(2):491–496.
19. Gao G, Schilling AF, Hubbell K, et al. Improved properties of bone and cartilage tissue from 3D inkjet-bioprinted human mesenchymal stem cells by simultaneous deposition and photocrosslinking in PEG-GelMA. *Biotechnol Lett.* 2015;37(11):2349–2355.
20. Christensen K, Xu C, Chai W, Zhang Z, Fu J, Huang Y. Freeform inkjet printing of cellular structures with bifurcations. *Biotechnol Bioeng.* 2015;112(5):1047–1055.
21. Gudapati H, Dey M, Ozbolat I. A comprehensive review on droplet-based bioprinting: past, present and future. *Biomaterials.* 2016;102:20–42.
22. Murphy SV, Atala A. 3D bioprinting of tissues and organs. *Nat Biotechnol.* 2014;32(8):773–785.
23. Guillotin B, Souquet A, Catros S, et al. Laser assisted bioprinting of engineered tissue with high cell density and microscale organization. *Biomaterials.* 2010;31(28):7250–7256.
24. Erben J, Jirkovec R, Kalous T, Klicova M, Chvojka J. The Combination of Hydrogels with 3D Fibrous Scaffolds Based on Electrospinning and Meltblown Technology. *Bioengineering (Basel).* 2022;9(11).
25. Zein I, Hutmacher DW, Tan KC, Teoh SH. Fused deposition modeling of novel scaffold architectures for tissue engineering applications. *Biomaterials.* 2002;23(4):1169–1185.

26. Ozbolat IT, Hospodiuk M. Current advances and future perspectives in extrusion-based bioprinting. *Biomaterials*. 2016;76:321–343.
27. Murphy SV, Skardal A, Atala A. Evaluation of hydrogels for bio-printing applications. *J Biomed Mater Res A*. 2013;101(1):272–284.
28. Yan Y, Wang X, Pan Y, et al. Fabrication of viable tissue-engineered constructs with 3D cell-assembly technique. *Biomaterials*. 2005;26(29):5864–5871.
29. Ouyang L, Yao R, Zhao Y, Sun W. Effect of bioink properties on printability and cell viability for 3D bioplotting of embryonic stem cells. *Biofabrication*. 2016;8(3):035020.
30. Colosi C, Shin SR, Manoharan V, et al. Microfluidic Bioprinting of Heterogeneous 3D Tissue Constructs Using Low-Viscosity Bioink. *Adv Mater*. 2016;28(4):677–684.
31. Gao Q, He Y, Fu JZ, Liu A, Ma L. Coaxial nozzle-assisted 3D bioprinting with built-in microchannels for nutrients delivery. *Biomaterials*. 2015;61:203–215.
32. Yeo M, Lee JS, Chun W, Kim GH. An Innovative Collagen-Based Cell-Printing Method for Obtaining Human Adipose Stem Cell-Laden Structures Consisting of Core-Sheath Structures for Tissue Engineering. *Biomacromolecules*. 2016;17(4):1365–1375.
33. Xie J, Li X, Xia Y. Putting Electrospun Nanofibers to Work for Biomedical Research. *Macromol Rapid Commun*. 2008;29(22):1775–1792.
34. de Ruijter M, Hrynevich A, Haigh JN, et al. Out-of-Plane 3D-Printed Microfibers Improve the Shear Properties of Hydrogel Composites. *Small*. 2018;14(8).
35. Castilho M, Feyen D, Flandes-Iparraguirre M, et al. Melt Electrospinning Writing of Poly-Hydroxymethylglycolide-co-epsilon-Caprolactone-Based Scaffolds for Cardiac Tissue Engineering. *Adv Healthc Mater*. 2017;6(18).
36. An BW, Kim K, Lee H, et al. High-Resolution Printing of 3D Structures Using an Electrohydrodynamic Inkjet with Multiple Functional Inks. *Adv Mater*. 2015;27(29):4322–4328.
37. Sun D, Chang C, Li S, Lin L. Near-field electrospinning. *Nano Lett*. 2006;6(4):839–842.
38. Hull CW. The Birth of 3D Printing. *Res-Technol Manage*. 2015;58(6):25–30.
39. Klimek L, Klein HM, Schneider W, Mosges R, Schmelzer B, Voy ED. Stereolithographic modelling for reconstructive head surgery. *Acta Otorhinolaryngol Belg*. 1993;47(3):329–334.
40. Nahmias Y, Arneja A, Tower TT, Renn MJ, Odde DJ. Cell patterning on biological gels via cell spraying through a mask. *Tissue Eng*. 2005;11(5–6).
41. Gauvin R, Chen YC, Lee JW, et al. Microfabrication of complex porous tissue engineering scaffolds using 3D projection stereolithography. *Biomaterials*. 2012;33(15):3824–3834.
42. Tang M, Xie Q, Gimple RC, et al. Three-dimensional bioprinted glioblastoma microenvironments model cellular dependencies and immune interactions. *Cell Res*. 2020;30(10):833–853.
43. Mei Y, Wu D, Berg J, et al. Generation of a Perfusable 3D Lung Cancer Model by Digital Light Processing. *Int J Mol Sci*. 2023;24(7).
44. Tiwari AP, Thorat ND, Priel S, Patil RM, Rohiwal S, Townley H. Bioink: a 3D-bioprinting tool for anticancer drug discovery and cancer management. *Drug Discov Today*. 2021;26(7):1574–1590.
45. Gungor-Ozkerim PS, Inci I, Zhang YS, Khademhosseini A, Dokmeci MR. Bioinks for 3D bioprinting: an overview. *Biomater Sci*. 2018;6(5):915–946.
46. Zuk PA, Zhu M, Ashjian P, et al. Human adipose tissue is a source of multipotent stem cells. *Mol Biol Cell*. 2002;13(12):4279–4295.
47. Ji S, Guvendiren M. Recent Advances in Bioink Design for 3D Bioprinting of Tissues and Organs. *Front Bioeng Biotechnol*. 2017;5:23.
48. Ooi HW, Mota C, Ten Cate AT, Calore A, Moroni L, Baker MB. Thiol-Ene Alginate Hydrogels as Versatile Bioinks for Bioprinting. *Biomacromolecules*. 2018;19(8):3390–3400.
49. Axpe E, Oyen ML. Applications of Alginate-Based Bioinks in 3D Bioprinting. *Int J Mol Sci*. 2016;17(12).
50. Shin SR, Zihlmann C, Akbari M, et al. Reduced Graphene Oxide-GelMA Hybrid Hydrogels as Scaffolds for Cardiac Tissue Engineering. *Small*. 2016;12(27):3677.
51. Lim KS, Schon BS, Mekhileri NV, et al. New Visible-Light Photoinitiating System for Improved Print Fidelity in Gelatin-Based Bioinks. *ACS Biomater Sci Eng*. 2016;2(10):1752–1762.
52. Ouyang L, Highley CB, Rodell CB, Sun W, Burdick JA. 3D Printing of Shear-Thinning Hyaluronic Acid Hydrogels with Secondary Cross-Linking. *ACS Biomater Sci Eng*. 2016;2(10):1743–1751.
53. Jang J, Kim TG, Kim BS, Kim SW, Kwon SM, Cho DW. Tailoring mechanical properties of decellularized extracellular matrix bioink by vitamin B2-induced photo-crosslinking. *Acta Biomater*. 2016;33:88–95.
54. Kao S, Mo J, Baird A, Eliceiri BP. Basic fibroblast growth factor in an animal model of spontaneous mammary tumor progression. *Oncol Rep*. 2012;27(6):1807–1814.
55. Mao XW, Kettering JD, Gridley DS. Immunotherapy with low-dose interleukin-2 and anti-transforming growth factor-beta antibody in a murine tumor model. *Cancer Biother*. 1994;9(4):317–327.
56. Jain RK. Tumor angiogenesis and accessibility: role of vascular endothelial growth factor. *Semin Oncol*. 2002;29(6 Suppl 16):3–9.
57. Dominici M, Le Blanc K, Mueller I, et al. Minimal criteria for defining multipotent mesenchymal stromal cells. The International Society for Cellular Therapy position statement. *Cytotherapy*. 2006;8(4):315–317.
58. Pittenger MF, Mackay AM, Beck SC, et al. Multilineage potential of adult human mesenchymal stem cells. *Science*. 1999;284(5411):143–147.
59. De Coppi P. Isolation of amniotic stem cell lines with potential for therapy. *Nat Biotechnol*. 2007;25(1):100–106.
60. Zhang YS, Xia Y. Multiple facets for extracellular matrix mimicking in regenerative medicine. *Nanomedicine*. 2015;10(5):689–692.
61. Cui H, Nowicki M, Fisher JP, Zhang LG. 3D Bioprinting for Organ Regeneration. *Adv Healthc Mater*. 2017;6(1).
62. Atala A, Kasper FK, Mikos AG. Engineering complex tissues. *Sci Transl Med*. 2012;4(160).
63. Place ES, Evans ND, Stevens MM. Complexity in biomaterials for tissue engineering. *Nat Mater*. 2009;8(6):457–470.
64. Pepelanova I. Tunable Hydrogels: introduction to the World of Smart Materials for Biomedical Applications. *Adv Biochem Eng Biotechnol*. 2021;178:1–35.
65. Chircov C, Grumezescu AM, Bejenaru LE. Hyaluronic acid-based scaffolds for tissue engineering. *Rom J Morphol Embryol*. 2018;59(1):71–76.
66. Kyle S, Jessop ZM, Al-Sabah A, Whitaker IS. ‘Printability’ of Candidate Biomaterials for Extrusion Based 3D Printing: state-of-The-Art. *Adv Healthc Mater*. 2017;6(16).
67. Kyburz KA, Anseth KS. Synthetic mimics of the extracellular matrix: how simple is complex enough? *Ann Biomed Eng*. 2015;43(3):489–500.

68. Crapo PM, Gilbert TW, Badylak SF. An overview of tissue and whole organ decellularization processes. *Biomaterials*. 2011;32(12):3233–3243.
69. Nagao RJ, Xu J, Luo P, et al. Decellularized Human Kidney Cortex Hydrogels Enhance Kidney Microvascular Endothelial Cell Maturation and Quiescence. *Tissue Eng Part A*. 2016;22(19–20):1140–1150.
70. Bi H, Ming L, Cheng R, Luo H, Zhang Y, Jin Y. Liver extracellular matrix promotes BM-MSCs hepatic differentiation and reversal of liver fibrosis through activation of integrin pathway. *J Tissue Eng Regen Med*. 2017;11(10):2685–2698.
71. Pati F, Jang J, Ha DH, et al. Printing three-dimensional tissue analogues with decellularized extracellular matrix bioink. *Nat Commun*. 2014;5:3935.
72. Shim JH, Kim JY, Park M, Park J, Cho DW. Development of a hybrid scaffold with synthetic biomaterials and hydrogel using solid freeform fabrication technology. *Biofabrication*. 2011;3(3):034102.
73. Huang G, Wang L, Wang S, et al. Engineering three-dimensional cell mechanical microenvironment with hydrogels. *Biofabrication*. 2012;4(4):042001.
74. Schuurman W, Levett PA, Pot MW, et al. Gelatin-methacrylamide hydrogels as potential biomaterials for fabrication of tissue-engineered cartilage constructs. *Macromol Biosci*. 2013;13(5):551–561.
75. Fan H, Wang L, Zhao K, et al. Fabrication, mechanical properties, and biocompatibility of graphene-reinforced chitosan composites. *Biomacromolecules*. 2010;11(9):2345–2351.
76. Riedl A, Schleiderer M, Pudelko K, et al. Comparison of cancer cells in 2D vs 3D culture reveals differences in AKT-mTOR-S6K signaling and drug responses. *J Cell Sci*. 2017;130(1):203–218.
77. Chitcholtan K, Asselin S, Sykes PH, Evans JJ. Differences in growth properties of endometrial cancer in three dimensional (3D) culture and 2D cell monolayer. *Exp Cell Res*. 2013;319(1):75–87.
78. Melissaridou S, Wiechec E, Magan M, et al. The effect of 2D and 3D cell cultures on treatment response, EMT profile and stem cell features in head and neck cancer. *Cancer Cell Int*. 2019;19:16.
79. Kelland LR. Of mice and men: values and liabilities of the athymic nude mouse model in anticancer drug development. *Eur J Cancer*. 2004;40(6):827–836.
80. Zhao Y, Shuen TWH, Toh TB, et al. Development of a new patient-derived xenograft humanised mouse model to study human-specific tumour microenvironment and immunotherapy. *Gut*. 2018;67(10):1845–1854.
81. Wang S, Gao D, Chen Y. The potential of organoids in urological cancer research. *Nat Rev Urol*. 2017;14(7):401–414.
82. Monteiro MV, Ferreira LP, Rocha M, Gaspar VM, Mano JF. Advances in bioengineering pancreatic tumor-stroma physiometric Biomodels. *Biomaterials*. 2022;287:121653.
83. Rodrigues J, Heinrich MA, Teixeira LM, Prakash J. 3D In Vitro Model (R)evolution: unveiling Tumor-Stroma Interactions. *Trends Cancer*. 2021;7(3):249–264.
84. Nanou A, Lorenzo-Moldero I, Gazouleas KD, Cortese B, Moroni L. 3D Culture Modeling of Metastatic Breast Cancer Cells in Additive Manufactured Scaffolds. *ACS Appl Mater Interfaces*. 2022;14(24):28389–28402.
85. Clevers H. Modeling Development and Disease with Organoids. *Cell*. 2016;165(7):1586–1597.
86. Murrow LM, Weber RJ, Gartner ZJ. Dissecting the stem cell niche with organoid models: an engineering-based approach. *Development*. 2017;144(6):998–1007.
87. Lancaster MA, Knoblich JA. Organogenesis in a dish: modeling development and disease using organoid technologies. *Science*. 2014;345(6194):1247125.
88. Zhou Y, Wang B, Wu J, et al. Association of preoperative EpCAM Circulating Tumor Cells and peripheral Treg cell levels with early recurrence of hepatocellular carcinoma following radical hepatic resection. *BMC Cancer*. 2016;16:506.
89. Murlidhar V, Reddy RM, Fouladdel S, et al. Poor Prognosis Indicated by Venous Circulating Tumor Cell Clusters in Early-Stage Lung Cancers. *Cancer Res*. 2017;77(18):5194–5206.
90. Hanahan D, Weinberg RA. Hallmarks of cancer: the next generation. *Cell*. 2011;144(5):646–674.
91. Nunes AS, Barros AS, Costa EC, Moreira AF, Correia JJ. 3D tumor spheroids as in vitro models to mimic in vivo human solid tumors resistance to therapeutic drugs. *Biotechnol Bioeng*. 2019;116(1):206–226.
92. Hanahan D, Coussens LM. Accessories to the crime: functions of cells recruited to the tumor microenvironment. *Cancer Cell*. 2012;21(3):309–322.
93. Mehta G, Hsiao AY, Ingram M, Luker GD, Takayama S. Opportunities and challenges for use of tumor spheroids as models to test drug delivery and efficacy. *J Control Release*. 2012;164(2):192–204.
94. Yamada KM, Cukierman E. Modeling tissue morphogenesis and cancer in 3D. *Cell*. 2007;130(4):601–610.
95. Ravi M, Paramesh V, Kaviya SR, Anuradha E, Solomon FD. 3D cell culture systems: advantages and applications. *J Cell Physiol*. 2015;230(1):16–26.
96. Roper SJ, Coyle B. Establishing an In Vitro 3D Spheroid Model to Study Medulloblastoma Drug Response and Tumor Dissemination. *Curr Protoc*. 2022;2(1):e357.
97. Lee SY, Hwang HJ, Lee DW. Optimization of 3D-aggregated spheroid model (3D-ASM) for selecting high efficacy drugs. *Sci Rep*. 2022;12(1):18937.
98. Lee DW, Kim JE, Lee GH, et al. High-Throughput 3D Tumor Spheroid Array Platform for Evaluating Sensitivity of Proton-Drug Combinations. *Int J Mol Sci*. 2022;23(2).
99. Li H, Liu P, Kaur G, Yao X, Yang M. Transparent and Gas-Permeable Liquid Marbles for Culturing and Drug Sensitivity Test of Tumor Spheroids. *Adv Healthc Mater*. 2017;6(13).
100. Popova AA, Tronser T, Demir K, et al. Facile One Step Formation and Screening of Tumor Spheroids Using Droplet-Microarray Platform. *Small*. 2019;15(25):e1901299.
101. Xia Y, Chen H, Li J, et al. Acoustic Droplet-Assisted Superhydrophilic-Superhydrophobic Microarray Platform for High-Throughput Screening of Patient-Derived Tumor Spheroids. *ACS Appl Mater Interfaces*. 2021;13(20):23489–23501.
102. Sabhachandani P, Motwani V, Cohen N, Sarkar S, Torchilin V, Konry T. Generation and functional assessment of 3D multicellular spheroids in droplet based microfluidics platform. *Lab Chip*. 2016;16(3):497–505.



103. Sabhachandani P, Sarkar S, McKenney S, Ravi D, Evens AM, Konry T. Microfluidic assembly of hydrogel-based immunogenic tumor spheroids for evaluation of anticancer therapies and biomarker release. *J Control Release*. 2019;295:21–30.
104. Berger Fridman I, Ugolini GS, VanDelinder V, Cohen S, Konry T. High throughput microfluidic system with multiple oxygen levels for the study of hypoxia in tumor spheroids. *Biofabrication*. 2021;13(3):48.
105. Deng Y, Liu SY, Chua SL, Khoo BL. The effects of biofilms on tumor progression in a 3D cancer-biofilm microfluidic model. *Biosens Bioelectron*. 2021;180:113113.
106. Kleinman HK, Martin GR. Matrigel: basement membrane matrix with biological activity. *Semin Cancer Biol*. 2005;15(5):378–386.
107. Kubota Y, Kleinman HK, Martin GR, Lawley TJ. Role of laminin and basement membrane in the morphological differentiation of human endothelial cells into capillary-like structures. *J Cell Biol*. 1988;107(4):1589–1598.
108. Lee SY, Teng Y, Son M, et al. Three-Dimensional Aggregated Spheroid Model of Hepatocellular Carcinoma Using a 96-Pillar/Well Plate. *Molecules*. 2021;26(16).
109. Chaudhuri O, Koshy ST, Branco da Cunha C, et al. Extracellular matrix stiffness and composition jointly regulate the induction of malignant phenotypes in mammary epithelium. *Nat Mater*. 2014;13(10):970–978.
110. Liu J, Tan Y, Zhang H, et al. Soft fibrin gels promote selection and growth of tumorigenic cells. *Nat Mater*. 2012;11(8):734–741.
111. Jeong SY, Lee JH, Shin Y, Chung S, Kuh HJ. Co-Culture of Tumor Spheroids and Fibroblasts in a Collagen Matrix-Incorporated Microfluidic Chip Mimics Reciprocal Activation in Solid Tumor Microenvironment. *PLoS One*. 2016;11(7):e0159013.
112. Charoen KM, Fallica B, Colson YL, Zaman MH, Grinstaff MW. Embedded multicellular spheroids as a biomimetic 3D cancer model for evaluating drug and drug-device combinations. *Biomaterials*. 2014;35(7):2264–2271.
113. Aisenbrey EA, Murphy WL. Synthetic alternatives to Matrigel. *Nat Rev Mater*. 2020;5(7):539–551.
114. Kim S, Min S, Choi YS, et al. Tissue extracellular matrix hydrogels as alternatives to Matrigel for culturing gastrointestinal organoids. *Nat Commun*. 2022;13(1):1692.
115. Kleinman HK, McGarvey ML, Hassell JR, et al. Basement membrane complexes with biological activity. *Biochemistry*. 1986;25(2):312–318.
116. Ng S, Tan WJ, Pek MMX, Tan MH, Kurisawa M. Mechanically and chemically defined hydrogel matrices for patient-derived colorectal tumor organoid culture. *Biomaterials*. 2019;219:119400.
117. Fang G, Lu H, Al-Nakashli R, et al. Enabling peristalsis of human colon tumor organoids on microfluidic chips. *Biofabrication*. 2021;14(1).
118. Jung DJ, Shin TH, Kim M, Sung CO, Jang SJ, Jeong GS. A one-stop microfluidic-based lung cancer organoid culture platform for testing drug sensitivity. *Lab Chip*. 2019;19(17):2854–2865.
119. Shirure VS, Bi Y, Curtis MB, et al. Tumor-on-a-chip platform to investigate progression and drug sensitivity in cell lines and patient-derived organoids. *Lab Chip*. 2018;18(23):3687–3702.
120. Tuveson D, Clevers H. Cancer modeling meets human organoid technology. *Science*. 2019;364(6444):952–955.
121. Ranga A, Girgin M, Meinhardt A, et al. Neural tube morphogenesis in synthetic 3D microenvironments. *Proc Natl Acad Sci U S A*. 2016;113(44):E6831–E6839.
122. Lancaster MA, Renner M, Martin CA, et al. Cerebral organoids model human brain development and microcephaly. *Nature*. 2013;501(7467).
123. Astashkina AI, Mann BK, Prestwich GD, Grainger DW. A 3-D organoid kidney culture model engineered for high-throughput nephrotoxicity assays. *Biomaterials*. 2012;33(18):4700–4711.
124. Takebe T, Sekine K, Enomura M, et al. Vascularized and functional human liver from an iPSC-derived organ bud transplant. *Nature*. 2013;499(7459):481–484.
125. Eiraku M, Takata N, Ishibashi H, et al. Self-organizing optic-cup morphogenesis in three-dimensional culture. *Nature*. 2011;472(7341):51–56.
126. Cruz-Acuna R, Quiros M, Farkas AE, et al. Synthetic hydrogels for human intestinal organoid generation and colonic wound repair. *Nat Cell Biol*. 2017;19(11):1326–1335.
127. Dye BR, Hill DR, Ferguson MA, et al. In vitro generation of human pluripotent stem cell derived lung organoids. *Elife*. 2015;4.
128. Chua CW, Shibata M, Lei M, et al. Single luminal epithelial progenitors can generate prostate organoids in culture. *Nat Cell Biol*. 2014;16(10):951–961, 951–954.
129. Ramachandran SD, Schirmer K, Munst B, et al. In Vitro Generation of Functional Liver Organoid-Like Structures Using Adult Human Cells. *PLoS One*. 2015;10(10):e0139345.
130. Ardalani H, Sengupta S, Harms V, Vickerman V, Thomson JA, Murphy WL. 3-D culture and endothelial cells improve maturity of human pluripotent stem cell-derived hepatocytes. *Acta Biomater*. 2019;95:371–381.
131. Gjorevski N, Lutolf MP. Synthesis and characterization of well-defined hydrogel matrices and their application to intestinal stem cell and organoid culture. *Nat Protoc*. 2017;12(11):2263–2274.
132. Cruz-Acuna R, Quiros M, Huang S, et al. PEG-4MAL hydrogels for human organoid generation, culture, and in vivo delivery. *Nat Protoc*. 2018;13(9):2102–2119.
133. Spence JR, Mayhew CN, Rankin SA, et al. Directed differentiation of human pluripotent stem cells into intestinal tissue in vitro. *Nature*. 2011;470(7332):105–109.
134. Sachs N, de Ligt J, Kopper O, et al. A Living Biobank of Breast Cancer Organoids Captures Disease Heterogeneity. *Cell*. 2018;172(1–2):373–386 e310.
135. Calandrini C, Schutgens F, Oka R, et al. An organoid biobank for childhood kidney cancers that captures disease and tissue heterogeneity. *Nat Commun*. 2020;11(1):1310.
136. Schuth S, Le Blanc S, Krieger TG, et al. Patient-specific modeling of stroma-mediated chemoresistance of pancreatic cancer using a three-dimensional organoid-fibroblast co-culture system. *J Exp Clin Cancer Res*. 2022;41(1):312.
137. Shi R, Radulovich N, Ng C, et al. Organoid Cultures as Preclinical Models of Non-Small Cell Lung Cancer. *Clin Cancer Res*. 2020;26(5):1162–1174.
138. Dost AFM, Moye AL, Vedaie M, et al. Organoids Model Transcriptional Hallmarks of Oncogenic KRAS Activation in Lung Epithelial Progenitor Cells. *Cell Stem Cell*. 2020;27(4):663–678 e668.
139. van de Wetering M, Francies HE, Francis JM, et al. Prospective derivation of a living organoid biobank of colorectal cancer patients. *Cell*. 2015;161(4):933–945.

140. Kopper O, de Witte CJ, Lohmussaer K, et al. An organoid platform for ovarian cancer captures intra- and interpatient heterogeneity. *Nat Med*. 2019;25(5):838–849.
141. Gao D, Vela I, Sboner A, et al. Organoid cultures derived from patients with advanced prostate cancer. *Cell*. 2014;159(1):176–187.
142. Bartfeld S, Bayram T, van de Wetering M, et al. In vitro expansion of human gastric epithelial stem cells and their responses to bacterial infection. *Gastroenterology*. 2015;148(1):126–136 e126.
143. Blanco-Fernandez B, Gaspar VM, Engel E, Mano JF. Proteinaceous Hydrogels for Bioengineering Advanced 3D Tumor Models. *Adv Sci (Weinh)*. 2021;8(4):2003129.
144. Nguyen DH, Stapleton SC, Yang MT, et al. Biomimetic model to reconstitute angiogenic sprouting morphogenesis in vitro. *Proc Natl Acad Sci U S A*. 2013;110(17):6712–6717.
145. Jimenez-Torres JA, Peery SL, Sung KE, Beebe DJ. LumeNEXT: a Practical Method to Pattern Luminal Structures in ECM Gels. *Adv Healthc Mater*. 2016;5(2):198–204.
146. Bai J, Haase K, Roberts JJ, et al. A novel 3D vascular assay for evaluating angiogenesis across porous membranes. *Biomaterials*. 2021;268:120592.
147. Winkler J, Abisoye-Ogunniyan A, Metcalf KJ, Werb Z. Concepts of extracellular matrix remodelling in tumour progression and metastasis. *Nat Commun*. 2020;11(1):5120.
148. Barbazan J, Matic Vignjevic D. Cancer associated fibroblasts: is the force the path to the dark side? *Curr Opin Cell Biol*. 2019;56:71–79.
149. Kalluri R. The biology and function of fibroblasts in cancer. *Nat Rev Cancer*. 2016;16(9):582–598.
150. Martino MM, Hubbell JA. The 12th–14th type III repeats of fibronectin function as a highly promiscuous growth factor-binding domain. *FASEB J*. 2010;24(12):4711–4721.
151. Mavrogomatou E, Pratsinis H, Papadopoulou A, Karamanos NK, Kleitsas D. Extracellular matrix alterations in senescent cells and their significance in tissue homeostasis. *Matrix Biol*. 2019;75–76:27–42.
152. Truong DD, Kratz A, Park JG, et al. A Human Organotypic Microfluidic Tumor Model Permits Investigation of the Interplay between Patient-Derived Fibroblasts and Breast Cancer Cells. *Cancer Res*. 2019;79(12):3139–3151.
153. Nagaraju S, Truong D, Mouneimne G, Nikkiah M. Microfluidic Tumor-Vascular Model to Study Breast Cancer Cell Invasion and Intravasation. *Adv Healthc Mater*. 2018;7(9):e1701257.
154. Nguyen DT, Lee E, Alimperti S, et al. A biomimetic pancreatic cancer on-chip reveals endothelial ablation via ALK7 signaling. *Sci Adv*. 2019;5(8):eaav6789.
155. Sun W, Chen Y, Wang Y, et al. Interaction study of cancer cells and fibroblasts on a spatially confined oxygen gradient microfluidic chip to investigate the tumor microenvironment. *Analyst*. 2018;143(22):5431–5437.
156. Jin MZ, Jin WL. The updated landscape of tumor microenvironment and drug repurposing. *Signal Transduct Target Ther*. 2020;5(1):166.
157. Brown JM, Wilson WR. Exploiting tumour hypoxia in cancer treatment. *Nat Rev Cancer*. 2004;4(6):437–447.
158. Jain RK. Normalization of tumor vasculature: an emerging concept in antiangiogenic therapy. *Science*. 2005;307(5706):58–62.
159. Kim H, Lin Q, Glazer PM, Yun Z. The hypoxic tumor microenvironment in vivo selects the cancer stem cell fate of breast cancer cells. *Breast Cancer Res*. 2018;20(1):16.
160. Wang M, Liu Y, Cheng Y, Wei Y, Wei X. Immune checkpoint blockade and its combination therapy with small-molecule inhibitors for cancer treatment. *Biochim Biophys Acta Rev Cancer*. 2019;1871(2):199–224.
161. Semenza GL. Targeting HIF-1 for cancer therapy. *Nat Rev Cancer*. 2003;3(10):721–732.
162. Lovett M, Lee K, Edwards A, Kaplan DL. Vascularization strategies for tissue engineering. *Tissue Eng Part B Rev*. 2009;15(3):353–370.
163. Bae H, Puranik AS, Gauvin R, et al. Building vascular networks. *Sci Transl Med*. 2012;4(160):160ps123.
164. Bates DO, Cui TG, Doughty JM, et al. VEGF165b, an inhibitory splice variant of vascular endothelial growth factor, is down-regulated in renal cell carcinoma. *Cancer Res*. 2002;62(14):4123–4131.
165. Sontheimer-Phelps A, Hassell BA, Ingber DE. Modelling cancer in microfluidic human organs-on-chips. *Nat Rev Cancer*. 2019;19(2):65–81.
166. Turley SJ, Cremasco V, Astarita JL. Immunological hallmarks of stromal cells in the tumour microenvironment. *Nat Rev Immunol*. 2015;15(11):669–682.
167. Muschler GF, Nakamoto C, Griffith LG. Engineering principles of clinical cell-based tissue engineering. *J Bone Joint Surg Am*. 2004;86(7):1541–1558.
168. Poldervaart MT, Gremmels H, van Deventer K, et al. Prolonged presence of VEGF promotes vascularization in 3D bioprinted scaffolds with defined architecture. *J Control Release*. 2014;184:58–66.
169. Kang HW, Lee SJ, Ko IK, Kengla C, Yoo JJ, Atala A. A 3D bioprinting system to produce human-scale tissue constructs with structural integrity. *Nat Biotechnol*. 2016;34(3):312–319.
170. Bertassoni LE, Cecconi M, Manoharan V, et al. Hydrogel bioprinted microchannel networks for vascularization of tissue engineering constructs. *Lab Chip*. 2014;14(13):2202–2211.
171. Gu J, Zhang Q, Geng M, et al. Construction of nanofibrous scaffolds with interconnected perfusable microchannel networks for engineering of vascularized bone tissue. *Bioact Mater*. 2021;6(10):3254–3268.
172. Liu W, Zhang YS, Heinrich MA, et al. Rapid Continuous Multimaterial Extrusion Bioprinting. *Adv Mater*. 2017;29(3).
173. Askari E, Seyfoori A, Amerreh M, et al. Stimuli-Responsive Hydrogels for Local Post-Surgical Drug Delivery. *Gels*. 2020;6(2).
174. Jungst T, Smolan W, Schacht K, Scheibel T, Groll J. Strategies and Molecular Design Criteria for 3D Printable Hydrogels. *Chem Rev*. 2016;116(3):1496–1539.
175. Stoltz JF, Zhang L, Ye JS, De Isla N. Organ reconstruction: dream or reality for the future. *Biomed Mater Eng*. 2017;28(s1):S121–S127.
176. Willemse J, van Tienderen G, van Hengel E, et al. Hydrogels derived from decellularized liver tissue support the growth and differentiation of cholangiocyte organoids. *Biomaterials*. 2022;284:121473.
177. Mollica PA, Booth-Creech EN, Reid JA, et al. 3D bioprinted mammary organoids and tumoroids in human mammary derived ECM hydrogels. *Acta Biomater*. 2019;95:201–213.
178. Schrader J, Gordon-Walker TT, Aucott RL, et al. Matrix stiffness modulates proliferation, chemotherapeutic response, and dormancy in hepatocellular carcinoma cells. *Hepatology*. 2011;53(4):1192–1205.



179. Sinha S, Ayushman M, Tong X, Yang F. Dynamically Crosslinked Poly(ethylene-glycol) Hydrogels Reveal a Critical Role of Viscoelasticity in Modulating Glioblastoma Fates and Drug Responses in 3D. *Adv Healthc Mater.* 2023;12(1):e2202147.
180. Yu M, Bardia A, Aceto N, et al. Cancer therapy. Ex vivo culture of circulating breast tumor cells for individualized testing of drug susceptibility. *Science.* 2014;345(6193):216–220.
181. Gao B, Yang Q, Zhao X, Jin G, Ma Y, Xu F. 4D Bioprinting for Biomedical Applications. *Trends Biotechnol.* 2016;34(9):746–756.
182. Gladman AS, Matsumoto EA, Nuzzo RG, Mahadevan L, Lewis JA. Biomimetic 4D printing. *Nat Mater.* 2016;15(4):413–418.

### International Journal of Nanomedicine

Dovepress

### Publish your work in this journal

The International Journal of Nanomedicine is an international, peer-reviewed journal focusing on the application of nanotechnology in diagnostics, therapeutics, and drug delivery systems throughout the biomedical field. This journal is indexed on PubMed Central, MedLine, CAS, SciSearch®, Current Contents®/Clinical Medicine, Journal Citation Reports/Science Edition, EMBase, Scopus and the Elsevier Bibliographic databases. The manuscript management system is completely online and includes a very quick and fair peer-review system, which is all easy to use. Visit <http://www.dovepress.com/testimonials.php> to read real quotes from published authors.

Submit your manuscript here: <https://www.dovepress.com/international-journal-of-nanomedicine-journal>